COASTAL LANDSLIDE AND SEA CLIFF RETREAT MONITORING FOR CLIMATE CHANGE ADAPTATION AND TARGETED RISK ASSESSMENT

Interim Report

PROJECT SPR 807

Oregon Department of Transportation

COASTAL LANDSLIDE AND SEA CLIFF RETREAT MONITORING FOR CLIMATE CHANGE ADAPTATION AND TARGETED RISK ASSESSMENT

Interim Report

PROJECT SPR 807

by
Michael J. Olsen,
Ben A. Leshchinsky,
Andrew Senogles,
Joan Herrmann,
and
Jonathan Allan

for

Oregon Department of Transportation
Research Section
555 13th Street NE, Suite 1
Salem OR 97301

and

Federal Highway Administration
1200 New Jersey Avenue SE
Washington, DC 20590

June 2022

Technical Report Documentation Page

1. Report No. FHWA-OR-RD-22-13	2. Government Accession No.	3. Recipient's Catalog No.
4. Title and Subtitle Coastal Landslide and Sea cliff Retreat Monitoring for Climate Change Adaptation and Targeted Risk Assessment		5. Report Date June 2022 6. Performing Organization Code
7. Author(s) Michael J. Olsen, ORCID 0000-0002-2989-5309 Ben A. Leshchinsky, ORCID 0000-0003-3890-1368 Andrew Senogles, ORCID 0000-0002-6607-2934 Joan Herrmann, and Jonathan Allan, ORCID 0000-0002-2303-3724		8. Performing Organization Report No.
9. Performing Organization Name and Address Oregon Department of Transportation Research Section 555 13th Street NE, Suite 1 Salem, OR 97301		10. Work Unit No. (TRAIS) 11. Contract or Grant No.
12. Sponsoring Agency Name and Address Oregon Dept. of Transportation Research Section 555 13th Street NE, Suite 1 Salem, OR 97301 Federal Highway Admin. 1200 New Jersey Avenue SE Washington, DC 20590		13. Type of Report and Period Covered Interim Report 14. Sponsoring Agency Code
15. Supplementary Notes		
16. Abstract: Though landslides and sea cliff erosion are common processes that damage Oregon's coastal highways regularly, sea cliff retreat and rate of movement are not well-characterized. The objective of this research project is to develop a more comprehensive, data-driven framework to prioritize coastal asset management, building on recent smaller-scale foundational efforts and recommendations. This interim report documents the progress to date by providing a summary of data acquisition and processing, sample results from preliminary analysis of the data, a risk framework model for progressive failure modeling incorporating climatic variables and enabling long-term projections along the shoreline, as well as highlights near-term benefits and applications for ODOT.		
17. Key Words Climate change, coastal erosion, sea cliffs, landslides, slope stability		18. Distribution Statement Copies available from NTIS, and online at http://www.oregon.gov/ODOT/Programs/Pages/Research-Publications.aspx

19. Security Classification (of this report) Unclassified	20. Security Classification (of this page) Unclassified	21. No. of Pages 81	22. Price

SI* (MODERN METRIC) CONVERSION FACTORS

APPROXIMATE CONVERSIONS TO SI UNITS

Symbol	When You Know	Multiply By	To Find	Symbol
		LENGTH		
in	inches	25.4	millimeters	mm
ft	feet	0.305	meters	m
yd	yards	0.914	meters	m
mi	miles	1.61	kilometers	km
		AREA		
in^2	square inches	645.2	millimeters squared	mm^2
ft^2	square feet	0.093	meters squared	m^2
yd^2	square yards	0.836	meters squared	m^2
ac	acres	0.405	hectares	ha
mi^2	square miles	2.59	kilometers squared	km^2
		VOLUME		
fl oz	fluid ounces	29.57	milliliters	ml
gal	gallons	3.785	liters	L
ft^3	cubic feet	0.028	meters cubed	m^3
yd^3	cubic yards	0.765	meters cubed	m^3
NOTE: Volumes greater than 1000 L shall be shown in m^3.				
		MASS		
oz	ounces	28.35	grams	g
lb	pounds	0.454	kilograms	kg
T	short tons (2000 lb)	0.907	megagrams	Mg
		TEMPERATURE (exact)		
°F	Fahrenheit	(F-32)/1.8	Celsius	°C

APPROXIMATE CONVERSIONS FROM SI UNITS

Symbol	When You Know	Multiply By	To Find	Symbol
		LENGTH		
mm	millimeters	0.039	inches	in
m	meters	3.28	feet	ft
m	meters	1.09	yards	yd
km	kilometers	0.621	miles	mi
		AREA		
mm^2	millimeters squared	0.0016	square inches	in^2
m^2	meters squared	10.764	square feet	ft^2
m^2	meters squared	1.196	square yards	yd^2
ha	hectares	2.47	acres	ac
km^2	kilometers squared	0.386	square miles	mi^2
		VOLUME		
ml	milliliters	0.034	fluid ounces	fl oz
L	liters	0.264	gallons	gal
m^3	meters cubed	35.315	cubic feet	ft^3
m^3	meters cubed	1.308	cubic yards	yd^3
		MASS		
g	grams	0.035	ounces	oz
kg	kilograms	2.205	pounds	lb
Mg	megagrams	1.102	short tons (2000 lb)	T
		TEMPERATURE (exact)		
°C	Celsius	1.8C+32	Fahrenheit	°F

*SI is the symbol for the International System of Measurement

ACKNOWLEDGEMENTS

The authors acknowledge the support of Dr. Kira Glover-Cutter, Curran Mohney, Geoff Crook, Mike Brinton, Katie Castelli, and Gary Pischke from ODOT as well as Adam Young from Scripps Institution of Oceanography at UCSD who have provided feedback on the project. Michael Bunn and Matt O'Banion (OSU PhD students) diligently prepared and installed the SAA MEMs sensors as well as developed the initial plans for the site surveys. Emerald Shirley (ODOT), Jill Dekoekkoek, and Pete Castro (ODOT) assisted with drilling and planning the Hooskanaden UAS surveys. Leica Geosystems and David Evans and Associates provided equipment and software used in this research. Maptek I-Site also provided software used in this study. The NSF Natural Hazards Engineering Research Infrastructure: Post-Disaster, Rapid Response Research (RAPID) Facility (Award CMMI-1611820) acquired and performed initial processing of the UUA lidar data to support this research. Special thanks to Jake Dafni, Michael Grilliot, and Andrew Lyda who executed those surveys. Joan Hermann (OSU) is assisting with the progressive seacliff failure analysis code and field work. Richie Slocum, Ezra Che, and Nick Matthews have helped with the field work.

DISCLAIMER

TABLE OF CONTENTS

LIST OF FIGURES

LIST OF TABLES

1.0 INTRODUCTION

1.1 BACKGROUND

Rising seas and extreme coastal weather events pose significant risks for the safety, reliability, and effectiveness of ODOT infrastructure and operations along the Oregon coast. Coastal landslides and cliff erosion are particularly sensitive to climate drivers with sea-level rise, storm frequency and intensity, wave scour, and rainfall amounts influencing landslide movement and sea cliff[1] erosion. The retreat rate of sea cliffs is also directly proportional to climate change effects and in many locations directly threatens disruption of ODOT's coastal infrastructure. Though landslides and sea cliff erosion are common processes that damage Oregon's coastal highways regularly (e.g., Figure 1.1), sea cliff retreat and rate of movement are not well-characterized. In 2014, ODOT's Coastal Climate Change Vulnerability Assessment identified this limited information regarding sea cliff retreat as an issue of concern.

Figure 1.1: Evidence of damage to Highway 101 at the Hooskanaden Slide requiring routine repaving of the road (MP344, August 2016).

[1] Coastal cliffs are steep slopes where the land and shoreline meet. They are often referred to as sea cliffs when adjacent to oceans and sea cliffs near lakes. However, the terms are often used interchangeably in practice. Please see Hampton et al. (2004) for further discussion. In this report, the term sea cliff is consistently used for clarity.

Considering that ODOT is designated as a lead implementation agency for the Governor's climate change adaptation priority, together with the observation that at least 26 sites totaling nearly 20 miles along Hwy 101 have already been identified as areas of concern, the need to assess landslides and coastal sea cliff retreat in terms of both magnitude and rate of movement and retreat will become increasingly critical. The rate and magnitude of sea cliff retreat are essential measures to be used in prioritizing highway segments situated upon those sea cliffs. These parameters would allow the agency to both prioritize sites for repair and financially plan for mitigation projects that are timed to maximize the utility of the existing facility. In this regard, the agency already knows which areas are impacted by sea cliff retreat, but without sufficient resources to address all of these locations at once, it becomes critical to determine which areas have the shortest lifespan so that they can be prioritized for repair. Research to directly address this concern is needed in order to optimize ODOT infrastructure planning, secure lifeline routes, and address the climate change adaptation focus of the Oregon Transportation Commission work plan.

The effects of sea cliff erosion and coastal landslide movements are of high social and economic relevance beyond the Pacific Northwest of the United States, as nearly one quarter of the global population lives in these areas (Small and Nicholls, 2003).

Previous coastal landslide research for ODOT includes investigation of the Johnson Creek Landslide and Arch Cape site in Lincoln and Clatsop counties, respectively. The Johnson Creek Landslide research study focused on the relationships between coastal sea cliff retreat, precipitation, and groundwater using standard survey methods to evaluate select cross-sectional areas of the coastal sea cliff at the toe of the landslide. A separate, brief analysis of the coastal sea cliff morphology of the Arch Cape site evaluated the use of terrestrial lidar (Light Detection and Ranging) technology for change detection. Compared to standard survey methods, terrestrial lidar provides a more accurate and efficient way to map, visualize, and quantify changes in coastal sea cliff erosion.

Though aerial-based lidar surveys conducted by the U.S. Army Corps of Engineers and DOGAMI/Oregon Lidar Consortium have been produced for coastal landscape-level use, the resolution is insufficient for what is needed to accurately monitor coastal sea cliff retreat. These sources also do not sufficiently capture the steep or vertical sea cliff faces, the shape of which directly affects erosion rates and subsequent slope movements. Furthermore, these surveys are not conducted with a sufficient frequency to enable meaningful temporal resolution of coastal sea cliff degradation. This temporal and topographic resolution is of particular importance to better understanding the timing and behavior of successive movements of coastal slopes after large storms, rainfall and erosion events.

In summary, given the limited research on coastal landslide movement and sea cliff retreat with respect to changing climate drivers, an increasingly long-term and in-depth monitoring study with modeling potential is critical to enable improved asset management decisions for ODOT, particularly in the face of climate change.

1.2 OBJECTIVES

The objective of SPR807 is to develop a more comprehensive, data-driven framework to prioritize coastal asset management. This new research for ODOT builds upon recent smaller-scale, foundational efforts, and recommendations. The primary objectives of this project are to:

1. Evaluate five representative sites reflecting a combination of coastal geologic terrains, landslide types, and sea cliff erosion activities.

2. Determine current geotechnical and hydrological data, as well as landslide and sea cliff geometry and movement using traditional and advanced 3D technologies (lidar and real-time remote in-place MEMS sensors).

3. Quantify changes in landslide movement, groundwater change, and sea cliff erosion rates over an extended 7-year timeline to fully capture the episodic nature of sea cliff erosion in the context of climate change events.

4. Develop a GIS/Lidar based management framework for targeted risk assessment and climate change adaptation planning including guidelines for future evaluations of coastal infrastructure sites.

1.3 SELECTED STUDY SITES

Five sites (Figure 1.2) were selected for this research: Arch Cape, Silver Point, Spencer Creek (Beverly Beach), Arizona Inn, and Hooskanaden. These sites are described in detail in the literature review provided to ODOT.

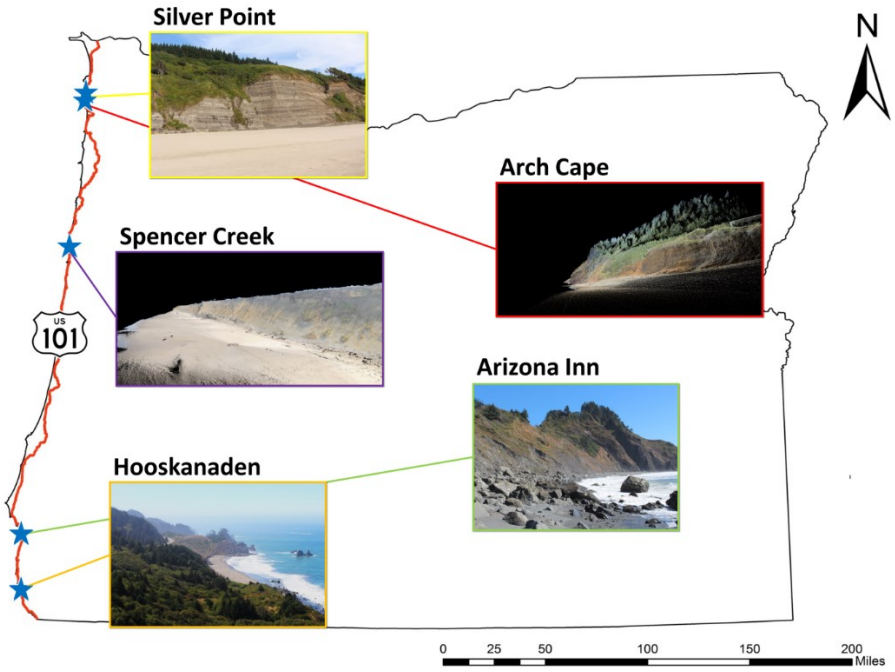

Figure 1.2: Map showing locations of the study sites.

1.4 DELIVERABLES TO DATE

In addition to regular quarterly reports and memos, the following major deliverables have been provided to ODOT:

- **Literature Review**: This document describes the geology and geohazards present along the Oregon Coast as well as provides general information on processes related to coastal landsliding and erosion. It then discusses monitoring technologies, slope stability analysis techniques, and coastal change analysis techniques. Relevant hazard mapping and erosion studies are also summarized. The review also provides background information such as geology specific to the sites that are being monitored as part of SPR-807.

- **Research Methodology**: The Research Methodology contains detailed, specific, standard operating procedures and business rules for systematic data acquisition, storage, processing, analysis to support the analysis and model development. Volume I covers the survey work to be completed as well as data gathering activities. Volume II is specific to the instrumentation installed on site.

- **Hooskanaden Preliminary Analysis**: Through supplemental funds, two Uncrewed Lidar Systems (ULS) datasets have been collected at Hooskanaden after a major failure in February 2019. One ULS dataset has been processed and delivered to ODOT as well as results from the preliminary analyses.

- **TAC Meetings**: Site selection and survey plans were reviewed at TAC meetings at the onset of the project.

- **Update Presentations** at the ODOT Geotechnical Engineering and Engineering Geology Technology Transfer Meetings. In 2017 and 2019, the research team has shared research results with ODOT personnel at these technology transfer meetings.

- **Publications:** Two scientific publications have resulted from this work. Copies of both have been provided to ODOT:

    - Leshchinsky, B., Olsen, M.J., Mohney, C., Glover-Cutter, K., Crook, G., Allan, J. Bunn, M.*, O'Banion, M.S.*, and Mathews, N. (2017). Mitigating coastal landslide damage, *Science*, 357(6355), 981-982. DOI: 10.1126/science.aao1722.

    - Leshchinsky, B., Olsen, M.J., Mohney, C. O'Banion, M.S.*, Bunn, M.*, Allan, J., and McClung, R. (2019). "A Framework for Quantifying Progressive Landslide Movement Stemming from Undercutting Processes and Hydrological Changes," Journal of Geophysical Research-Earth Surface, 124(2), 616-638. AGU. https://doi.org/10.1029/2018JF004833

1.5 SCOPE OF THE DOCUMENT

This interim report documents the progress to date by providing a summary of data acquisition and processing, sample results from preliminary analysis of the data, a risk framework model for progressive failure modeling incorporating climatic variables and enabling long-term projections along the shoreline, as well as highlights near-term benefits and applications for ODOT.

2.0 DATA COLLECTION AND INSTRUMENTATION PROGRESS TO DATE

This chapter summarizes the data collected thus far in the project, as well documents the various field activities that are being completed in this project. It also describes data processing efforts. This chapter also contains details regarding recent UAS lidar surveys conducted at the Arizona Inn and Hooskanaden sites. Lastly, this chapter contains information about status of the instrumentation installed at each site.

In order to maintain consistent data collections throughout the seven-year project, at the onset of the project site plan posters summarizing the data collection to take place at each site were created. These plan posters contain useful information such as: scan position locations, GNSS base station setup positions, total station setup positions, total station survey markers, current and new MEMs sensor positions, and other useful logistical information about each site. These posters can be found in Figure 2.1 through Figure 2.5 for the sites studied.

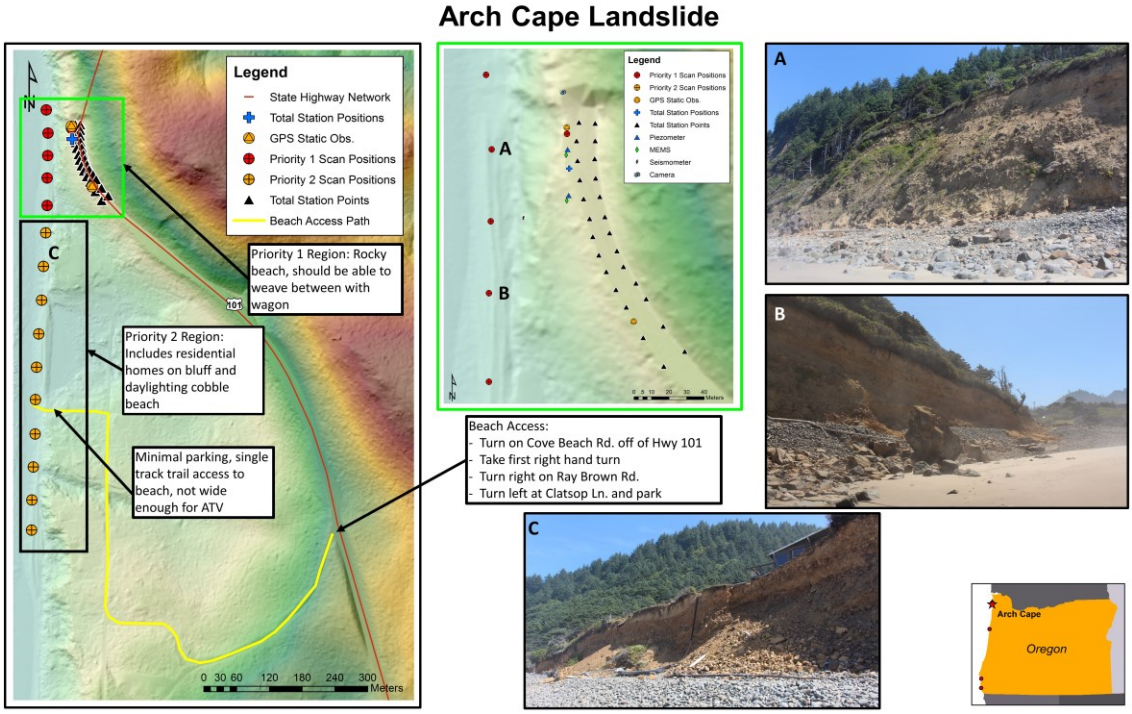

Figure 2.1: Site poster of Arch Cape created displaying: Scan positions, GNSS base setup positions, total station setups and other useful information about the site.

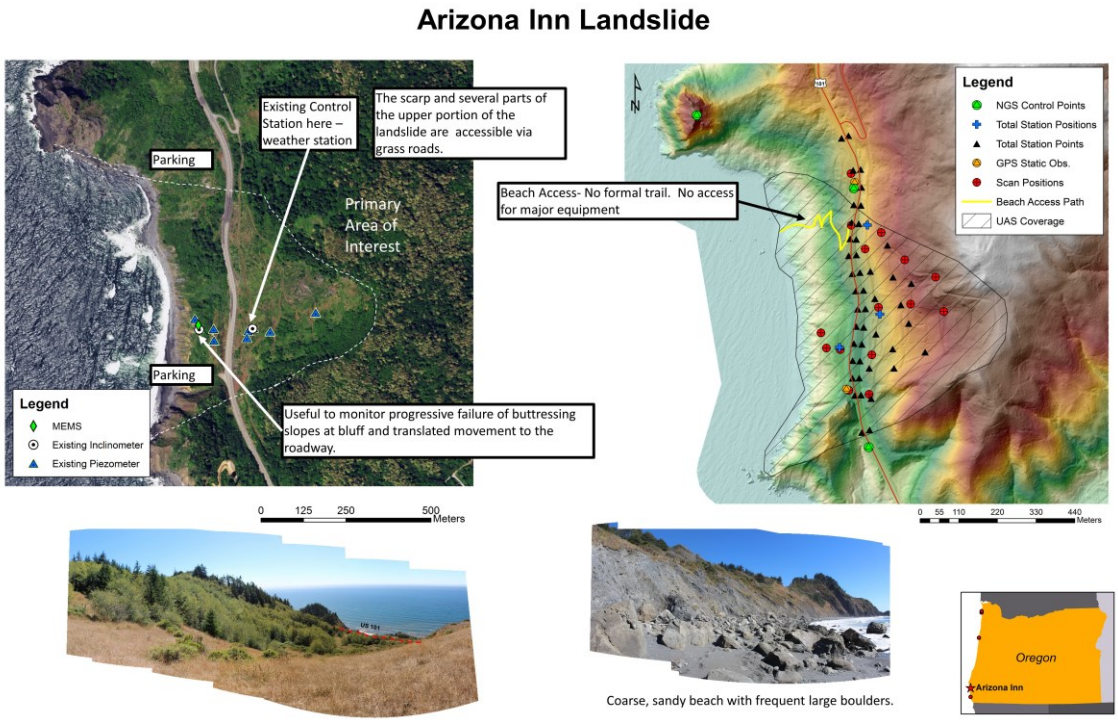

Figure 2.2: Site poster of Arizona Inn created displaying: Scan positions, GNSS base setup positions, total station setups and other useful information about the site.

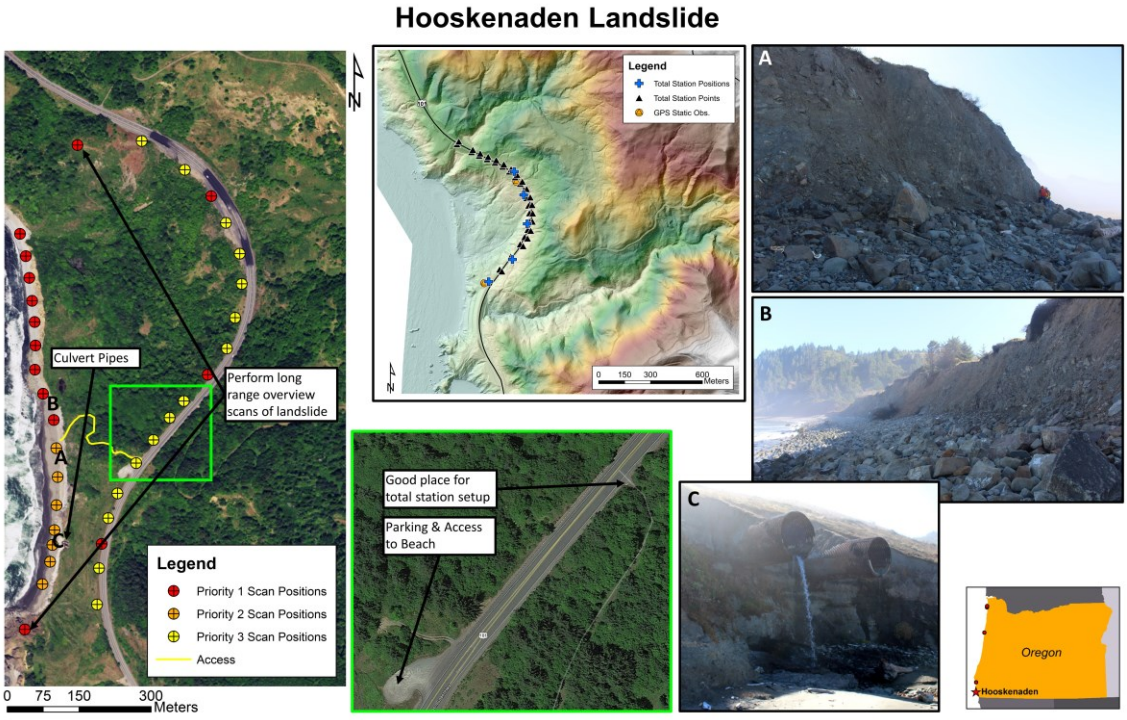

Figure 2.3: Site poster of Hooskanaden created displaying: Scan positions, GNSS base setup positions, total station setups and other useful information about the site.

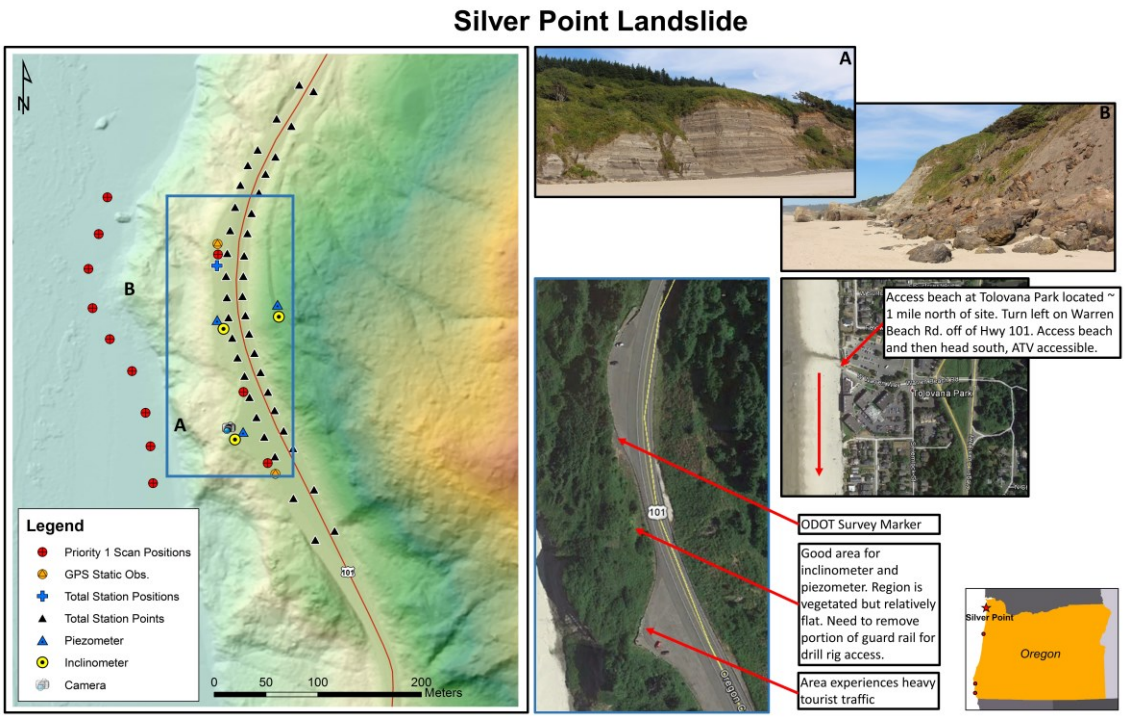

Figure 2.4: Site poster of Silver Point created displaying: Scan positions, GNSS base setup positions, total station setups and other useful information about the site.

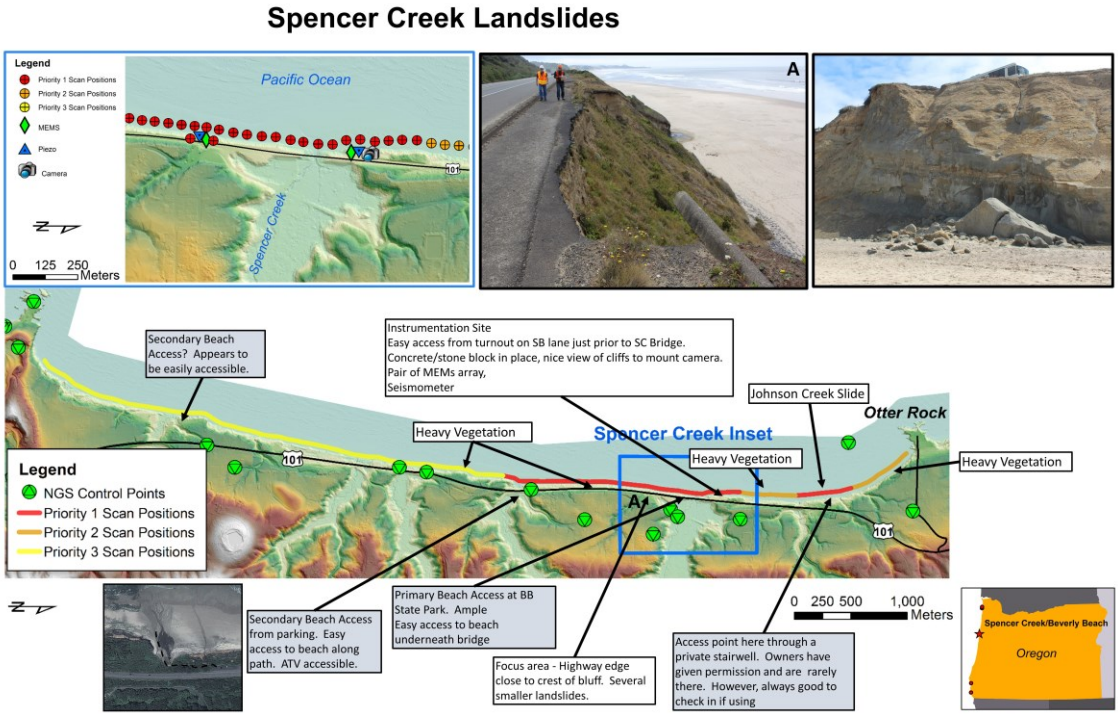

Figure 2.5: Site poster of Spencer Creek created displaying: Scan positions, MEM's positions, and other useful information about the site.

2.1 STATUS OF DATA COLLECTION AND PROCESSING

As set out in the work plan, bi-annual lidar surveys have been conducted out at all five sites during the fall and spring months in order to capture data relating to changes over the summer (expected accretion) and winter (expected erosion) months. Table 2.1 through Table 2.5 summarize the survey work conducted at each site at the time of writing (October 2019). All data collected as of August 2019 (with the exception of the UAS lidar surveys in June 2019) has been processed including data backup, georeferencing, exporting to standard pointcloud formats (.las or .e57), and cropping to the area of interest. Given the volatile environment that is being surveyed in this project, there are some small gaps/missing data at some of the sites, especially in the beginning of the project when some of the methods and field plan were still being refined. This information, along with survey dates and types are summarized in the Table 2.1 through

Table 2.5 below as well as outlined in sections 2.0 and 2.1.2 below.

Table 2.1: Table Summarizing Data Collected and Processed at Arch Cape.

ARCH CAPE					
Survey epoch	**Survey date**	**Scanner used**	**Total station**	**Processed**	**Comment**
2016 Fall	09/07/2016	VZ-400	N/A	Yes	
2017 Spring	06/02/2017	VZ-400	Yes	Yes	Only five scans collected
2017 Fall	10/09/2017	VZ-400	Yes	Yes	No scans collected
2018 Spring	05/17/2018	VZ-400, BLK360	N/A	Yes	Total station malfunction
2018 Fall	10/09/2018	VZ-400, BLK360	Yes	Yes	
2019 Spring	05/09/2019	VZ-400	Yes	Yes	No RGB in scans
2019 Fall	09/29/2019	VZ-400	Yes	Yes	

Table 2.2: Table Summarizing Data Collected and Processed at Arizona Inn.

Survey epoch	Survey date	Scanner used	Total station	UAS	Comment
2016 Fall	10/19/2016	VZ-400	N/A	Exom Alibris	
2017 Spring	06/14/2017	P40	Yes	N/A	
2017 Fall	11/27/2017	VZ-400	N/A	N/A	
2018 Spring	06/18/2018	VZ-400	Yes	N/A	
2018 Fall	10/15/2018	VZ-400	N/A	N/A	
2019 Spring	06/24/2019	VZ-400	N/A	PLS Mini ranger lidar + DJI P4P RTK	No RGB in scans
2019 Fall	10/03/2019	VZ-400	N/A	DJI P4P RTK	

Table 2.3: Table Summarizing Data Collected and Processed at Hooskanaden.

Survey epoch	Survey date	Scanner used	Total station	UAS	Comment
2016 Fall	10/18/2016	VZ-400	N/A	N/A	
2017 Spring	06/12/2017	P40	Yes	N/A	
2017 Fall	11/28/2017	VZ-400	Yes	N/A	No Beach Scans
2018 Spring	06/19/2018	VZ-400, BLK 360	Yes	N/A	
2018 Fall	10/16/2018	VZ-400	N/A	N/A	
2019 Spring	03/02/2019	VZ-400	N/A	DJI P4P RTK	No Beach Scans
	03/15/2019	VZ-400	N/A	Mini ranger lidar	No RGB in scans
	06/24/2019	VZ-400, BLK 360	N/A	Mini ranger lidar + DJI P4P	No RGB in scans
2019 Fall	10/04/2019	VZ-400, BLK 360	N/A	DJI P4P RTK	

Table 2.4: Table Summarizing Data Collected and Processed at Silver Point.

SILVER POINT					
Survey epoch	**Survey date**	**Scanner used**	**Total station**	**Processed**	**Comment**
2016 Fall	09/07/2016	VZ-400	N/A	Yes	
2017 Spring	06/01/2017	VZ-400	Yes	Yes	
2017 Fall	10/09/2017	VZ-400	Yes	Yes	
2018 Spring	05/17/2018	VZ-400	N/A	Yes	Total station malfunction
2018 Fall	10/09/2018	VZ-400	Yes	Yes	
2019 Spring	05/09/2019	VZ-400	Yes	Yes	No RGB in scans
2019 Fall	09/28/2019	VZ-400	Yes	Yes	

Table 2.5: Table Summarizing Data Collected and Processed at Spencer Creek.

SPENCER CREEK				
Survey epoch	**Survey date**	**Scanner used**	**Processed**	**Comment**
2016 Fall	09/22/2016	VZ-400	Yes	
2016 Fall	11/04/2016	VZ-400	Yes	
2017 Spring	05/08/2017	VZ-400	Yes	
2017 Fall	09/28/2017, 10/03/2017	VZ-400	Yes	
2018 Spring	04/26/2018, 05/16/2018	VZ-400	Yes	
2018 Fall	11/08/2018	VZ-400	Yes	
2019 Spring	05/31/2019	VZ-400	Yes	No RGB in scans
2019 Fall	10/10/2019	VZ-400	Yes	

2.1.1 Issues encountered in the field work

As mentioned above, several issues have periodically impeded the field data collection at particular sites. Some of these issues have resulted in an adaptation and change to the original fieldwork plan outlined in the previously submitted methodology. Those are highlighted in section 2.1.2 below.

- In spring of 2017 there was an incident with carrying the Riegl VZ-400 at the Arch Cape site across slick rocks during the field survey which resulted in only five TLS

scans being collected at this site, and the P40 TLS having to be used at other sites for this epoch.

- In fall of 2017 a sneaker wave damaged the battery being used to power the Riegl VZ-400 at the Arch Cape site during the field survey and as a result no beach scans were collected. Also, a large swell occurred during the Hooskanaden survey, rendering the beach inaccessible to the survey crew.

- In spring of 2018 a malfunction occurred with the total station during the north coast surveys (Arch Cape and Silver Point); hence, no total station measurements were obtained.

- In spring of 2019, the camera connection port for the Riegl VZ-400 malfunctioned, and as a result none of the scans surveyed in the spring 2019 epoch contain RGB values. In summer of 2019 the Riegl VZ-400 and camera were sent to the manufacturer for repair, maintenance, and re-calibration. Full operation was restored for the Fall 2019 surveys.

- Total station observations were discontinued at the faster moving landslide sites (Arizona Inn and Hooskanaden) after Spring 2018. Given the frequent repairs and maintenance at the site, the hubs used for monitoring were frequently lost. However, many objects such as telephone poles and guardrails serve as similar reference points and movements can be extracted from the TLS data.

2.1.2 Modifications to field collection from initial plan

As a result of the narrow beach issues encountered at the Arch Cape and Hooskanaden, the BLK360 TLS is now being utilized at these sites to collect data in conjunction with the Riegl VZ-400 when the tide results in a narrow beach during field work (Figure 2.6). This provides the following three benefits:

1. Fewer scans are required with the bulkier, more expensive VZ-400 which reduces the operation time in the hazardous tidal zone.

2. Scans can be conducted at closer spacing and closer to the sea cliff and farther from the waves without dramatically increasing the survey duration.

3. The light weight and simple setup of the BLK (no external batteries) allows it to be easily removed from harm's way in the event of a sneaker wave or other situation.

The BLK360 scans are registered to the Riegl VZ-400 scans (which are constrained to RTK GNSS positions) during processing using a cloud to cloud registration algorithm in order to georeferenced the scans. This process has been outlined in depth in an updated version of the methodology.

At the two south coast sites (Arizona Inn and Hooskanaden) problems have been encountered with the envisioned total station – road alignment survey strategy. While this part of the project

was not outlined in the original workplan, plans were made to conduct these measurements at the south coast (Arizona Inn and Hooskanaden) and north coast (Arch Cape and Silver Point) sites in order to track any movements in the road at a more precise level than TLS scans. Given the rapid movement of the south coast landslides, the road surfaces are continually repaved, resulting in frequent removal of PK nail control points that were set to monitor the road. As a result, most of these markers are lost before they can be resurveyed. Any replacement PK nails are also quickly removed. However, given the large changes taking place at these sites, and the success of the TLS surveys, the decision was made to remove this part of the survey from the south coast sites, and spend more time conducting extra TLS scans. Additional scans are now performed on the upper portion of the Hooskanaden landslide and the Arizona Inn landslide. To further supplement the data collection at these active sites, additional UAS SfM/MVS photogrammetric data is now being collected at the south coastal sites using OSU's recently purchased DJI Phantom 4 Pro (P4P) UAS system. The UAS system enables us to capture orthomosaics across the entire slide as well as generate SfM/MVS photogrammetric point clouds that can be combined with the TLS data to model the site.

Figure 2.6: Photograph of the BLK360 TLS (terrestrial laser scanner) being used to survey the sea cliff at the Hooskanaden beach during the bi-annual field survey on Oct 4, 2019.

2.2 UAS LIDAR AND SFM/MVS SURVEYS

After the destructive Hooskanaden landslide event in February 2019, we quickly mobilized to the site and conducted repeat TLS scans (Figure 2.7) and UAS SfM/MVS photogrammetric flights on the actively moving landslide on the weekend of March 2, 2019. Several weeks later the OSU team collaborated with the NSF Natural Hazards Research Infrastructure (NHERI) RAPID Facility team at the University of Washington to conduct UAS lidar surveys at Hooskanaden using their Phoenix miniRanger UAS lidar system (Figure 2.8) as well as collect additional TLS scans to serve as validation. This survey was conducted on the weekend of March 15, 2019. These surveys were conducted as bonus surveys to provide data associated with the Hooskanaden landslide event (Figure 2.9). An additional UAS lidar survey was performed later during the regular spring survey (week of June 24, 2019). This was also performed in collaboration with the RAPID Facility with flights conducted at both the Arizona Inn and Hooskanaden sites. Additional UAS SfM/MVS photogrammetric flights were conducted using the DJI Phantom 4 pro as well as the regular TLS survey. Preliminary analysis from data associated with the Hooskanaden landslide event as well as UAS lidar data is described in Section 3.2.

Figure 2.7: Photograph of Riegl VZ-400 TLS setup to conduct high resolution repeat scans of the actively moving Hooskanaden landslide on March 2, 2019.

Figure 2.8: Photograph capturing the RAPID Facility's phoenix lidar miniRanger UAS lidar system being operated at the Hooskanaden landslide on March 15, 2019. Photo Credit: Nick Mathews (OSU).

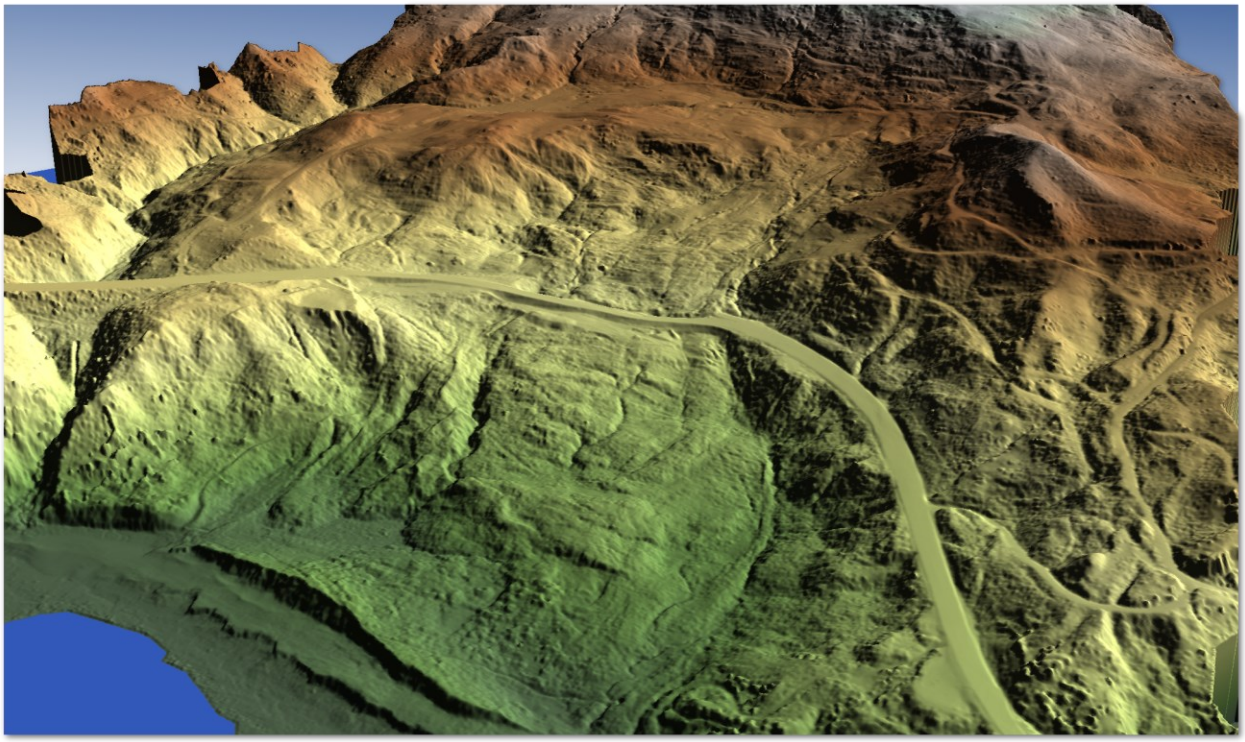

Figure 2.9: Example 3D view of the final 0.5m DEM created from data collected by the UAS lidar survey conducted at the Hooskanaden landslide from March 15, 2019. (Image Credit: Benjamin Babbel (OSU))

2.3 INSTRUMENTATION INSTALLATION AND STATUS

After the selection of the sites, visits to the sites were conducted to verify the proposed locations for drilling boreholes to install the instrumentation. MEMs (consisting of Measurand Shape Accel Array (SAA) systems) and piezometer sensors were installed in the drilled boreholes at Arch Cape, Arizona Inn, Silver Point and Spencer Creek during the winter of 2016/2017. The same system was then installed at Hooskanaden in late November 2017. Figure 2.10 shows the drill rig utilized for the drilling for this project, whilst Figure 2.11 shows an example of the borehole cores recovered from drilling providing additional information about each of the landslides. After drilling was complete to the planned depth, SAA MEMs and piezometer sensors were installed into the hole. Accelerometers are spaced every meter on the SAA MEMs. Two piezometers were installed at each site below the water table at different elevations. The housing for the electrical components (Figure 2.12) was then installed at the site with concrete and a steel post as shown in Figure 2.13.

The SAA installed at Hooskanaden stopped reporting data after it sheared in January 2018 after approximately 150mm of movement in the two months the system was installed (approximately 3mm/day). The SAA at Arizona Inn stopped reporting data after it sheared in March 2019 with a cumulative total of 80mm of movement. The SAA systems and piezometers installed at Arch Cape, Silver Point and Spencer creek (both north and south) are still fully operational as of the writing of this report (January 2020).

Figure 2.10: Drill rig actively drilling borehole for SAA MEM's installation at Arch Cape on January 20, 2017. Photograph Credit: Dr Michael Bunn.

Figure 2.11: Example borehole cores recovered from Arizona Inn during drilling on February 2, 2017. Photograph Credit: Dr Michael Bunn.

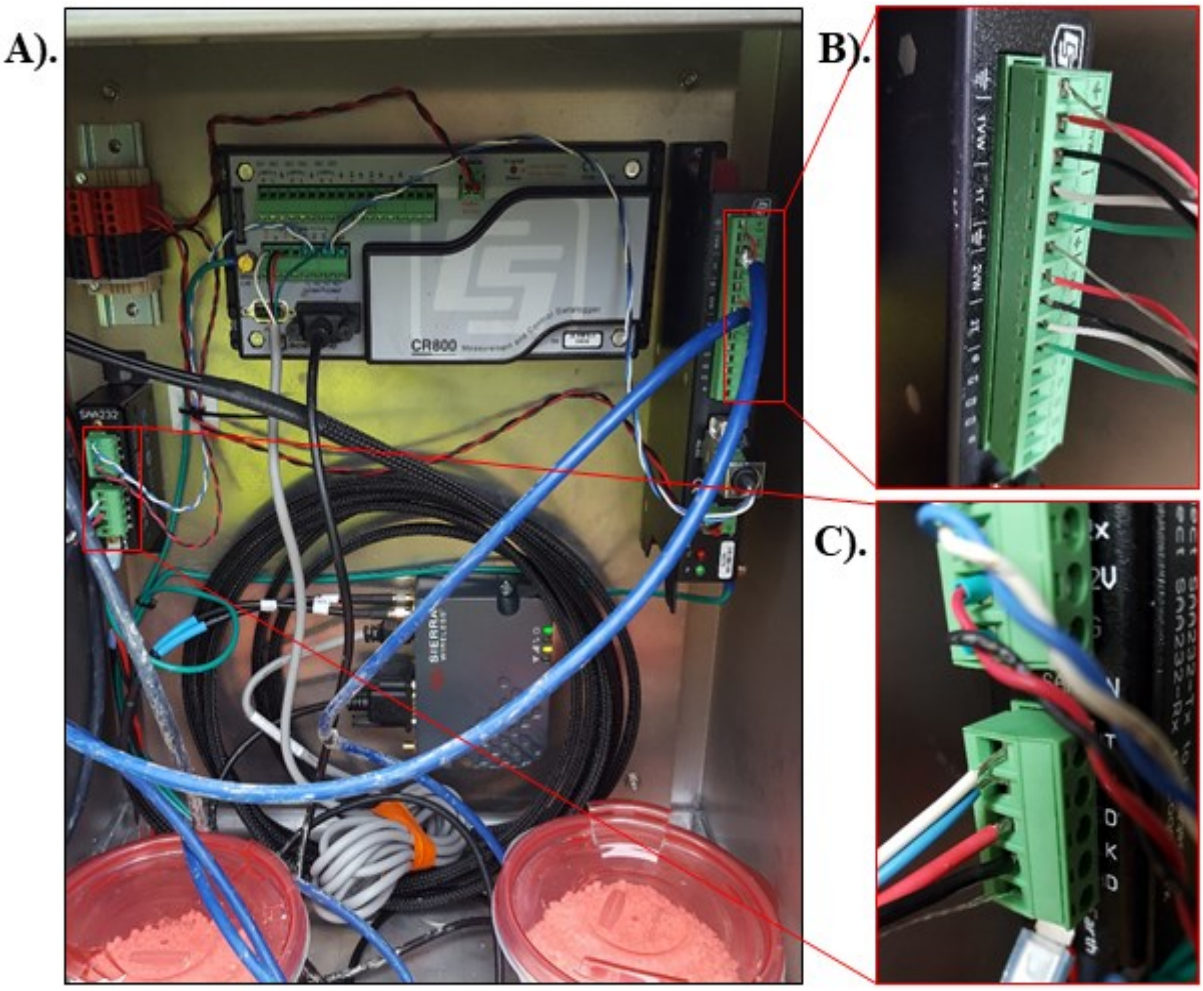

Figure 2.12: Electronics used to operate the SAA sensor. A). Overview of electronic components contained in the weatherproof casing including data logger and wireless modem. B). Pore pressure transducer multiplexer. C). SAA multiplexer. Photograph Credit: Dr Michael Bunn.

Figure 2.13: Final SAA MEM's sensor setup at Spencer Creek on January 27, 2017. Composed of solar panel for power supply, SAA electrical components (top box), SAA battery (bottom box), and SAA sensor (in borehole). Photograph Credit: Dr Michael Bunn.

2.4 COMPILATION OF TIDE DATA

As described in the research methodology tidal data is being archived from the NOAA website for the following tidal stations to capture wave effects impacting the sea cliffs:

- Garibaldi, OR
- South Beach, OR
- Port Orford, OR

Initially, this data has been used in comparison with the SAA/piezometer data due to the similar temporal resolution (see Figure 3.23 as an example from Arch Cape). These data can also be condensed into intervals between survey epochs to compare the relationship between tidal levels and erosion once more survey data is available.

2.5 INSTALLATION OF RTK GNSS SENSORS (IN PROGRESS)

On-site instrumentation is essential to understand the kinematics of landslides. However, subsurface instrumentation will no longer perform once sheared by a moving slide. Arizona Inn and Hooskanaden Landslides were instrumented as part of ODOT Research SPR807 and SPR808, representing active landslides that threaten much of Southern HWY101 in Oregon.

These landslides move yearly as a result of rainfall and significant coastal erosion. Just recently, Hooskanaden began its most remarkable failure in decades, moving over 150 feet since the onset of failure on 2/25/2019 after almost a foot of rain in 24 hours, and the slide continued to move substantially several weeks after the main event. The rapid movement as well as the failure of this magnitude has resulted in shearing of the installed subsurface instrumentation and closure of HWY101 with no effective means of quantitatively monitoring its movements through traditional geotechnical instrumentation. A quick hit research and STIC supplemental funding to SPR807 is piloting recent advances in low-cost surface geospatial monitoring technologies (Global Navigation Satellite System Real Time kinematic, GNSS RTK) to monitor landslide movement for both Hooskanaden and Arizona Inn under conditions where subsurface investigation and monitoring is no longer ideal. The Open Sensors Lab at OSU has built a system called Slide Sentinel that consists of a GNSS base, several RTK GNSS receivers with accelerometers as nodes, and the supporting communication system. These sensors are relatively low cost compared (few thousand $US) with the more traditional survey RTK GNSS sensors ($10-15k US). The OSU team is improving and testing the design and setup.

The Arizona Inn and Hooskanaden landslides were instrumented with state-of-the-art geotechnical monitoring systems by OSU – including both MEMS inclinometers, conventional piezometers and dataloggers, sending data back to OSU every half hour for analysis and interpretation. For both landslides, the shear zone has now been identified, a critical step in understanding the mechanics of a landslide. However, owing to the large internal deformations of these landslides, this instrumentation has now failed. Hooskanaden's monitoring system (installed in 2017 for SPR 808) sheared within 2.5 months due to its significant movement even prior to its recent dramatic failure. Arizona Inn's system (installed in 2016 for SPR 807) saw progressive seasonal movements for its first two years until a bluff collapse in January 2019, after which it advanced relatively quickly. Owing to heavy rainfall, the same day that Hooskanaden began to fail catastrophically, the Arizona Inn landslide moved so much that its instruments have now also sheared and failed. This landslide, previously fixed in 1996, is beginning to show renewed signs of distress and instability and is a potential upcoming threat to mobility on HWY101. The current challenge of collecting long-term landslide monitoring data within large earthflows that traverse HWY101 on the South Coast of Oregon is the physical limitation (breakage) of subsurface instruments during high landslide activity.

Based on the work to date on SPR 807 and prior efforts by ODOT, long-term geotechnical monitoring of these two highly active landslides is not practical nor safe. However, by using a rapidly deployable system of small, inexpensive RTK GNSS units, ODOT may leverage real-time data to monitor slide movements without the concern of losing instrumentation under significant ground distress. Such a system has been employed successfully in numerous slides (e.g. Gili et al 2000, Squarzoni et al. 2005, Benoit et al. 2015, etc.), and would enable high temporal resolution for landslide velocities with increased spatial resolution by deploying several nodes throughout the landslide mass. Supplemented with change detection using high-resolution lidar and photogrammetric techniques, which are already ongoing, we may increase spatial resolution of change. Thus, we may corroborate slide movement vectors between GNSS units, which have better survey control in both horizontal and vertical directions. Change detection has been demonstrated to be a reasonable means of estimating landslide distress, demonstrated by the project team for the Spangler landslide in 2018-2019; however, challenges such as vegetation and survey control may limit its accuracy. These monitoring efforts are also limited in terms of

temporal resolution. RTK GNSS enables more continuous tracking of landslide movements than repeat UAS or TLS lidar surveys.

2.5.1 Research tasks

Towards this end, the research team is completing the following tasks:

1. Acquire and customize rapidly deployable RTK GNSS units. Install systems at Hooskanaden and Arizona Inn landslides. Work with ODOT Geometronics for survey control, coordination, and implementation recommendations.

2. Leverage past monitoring of slope failures and erosion from SPR807 and SPR808 to corroborate RTK GNSS and lidar change detection measurements. Knowledge of the slide plane observed from in situ monitoring will supplement observed surface movements and enable interpretation of slide kinematics.

3. Create a framework and guidance for reconstructing slide dynamics and plausible slide planes based on surface movement trajectories.

4. Corroborate relationship between ongoing monitoring of rainfall and coastal erosion with landslide movements, relevant to both SPR807 and SPR808.

5. Provide recommended guidance for GNSS RTK rapid deployment for future landslides impacting ODOT infrastructure.

Currently, the research team is working with the Open Sensors lab to customize the RTK GNSS sensors and hardware components to optimize their use for the large landslides. We have also conducted tests to evaluate the data quality of these sensors. The sensors will be deployed to the field sites for testing in the near future (by March 2020).

2.5.2 Implementation and significance

Deployment of a GNSS RTK system will provide long-term, continual landslide monitoring data critical to SPR 807, SPR 808 and Region 3, while also showcasing a potential technology transfer that may enable ODOT to have significant cost-savings through augmenting the cost of extensive drilling and geotechnical monitoring. In lieu of subsurface instrumentation lost to these two active slides, this research will support the monitoring needs that are a part of ODOT Research Projects SPR 807 and SPR 808, as well as provide guidance for and proof-of-concept of these supplementary surface monitoring techniques for ODOT. In the case of landslides that exhibit significant seasonal movements – e.g., many of the landslides on Oregon's South Coast – GNSS RTK may be the only viable means of long-term monitoring of landslide kinematics. Understanding landslide kinematics assists ODOT with planning for mitigation to avoid or at least prepare for the next slide closure of our highway systems.

3.0 DATA ANALYSIS PROGRESS TO DATE

This chapter provides sample results from preliminary analyses of the data that have been collected at all five of the sites thus far. This analysis includes general analysis techniques performed across all the sites thus far (change detection for sea cliff retreat, SAA movement analysis, etc.) as well as site specific analysis to look into some of the unique challenges that each site presents in terms of slope stability problems.

3.1 TLS ANALYSIS RESULTS AT SITE

In order to create consistent and accurate change detection models over the seven-year study period of this project, a detailed methodology was created (See research methodology Volume 1 for details). Since this document was created the following changes have been made to the TLS analysis methodology:

1. Pre analysis modelling utilizes Cloud Compare visualization/functions rather than Leica Cyclone and has been partially scripted for efficiency.

2. Bounding boxes defining the area of interest have been created for each site in order to ensure a consistent area is being examined each time.

3. 3D polylines have been created to define the sea cliff extents. This ensures consistent cropping and removal of features above and below the sea cliff (trees, beach sand, etc.).

4. Large objects which are not part of the sea cliff (trees, vegetation, etc.) are manually cropped using Cloud Compare.

5. Files are then exported as .las files (previously .txt) and converted to .bpd files for analysis is RAMBO.

6. RAMBO is then used to perform functions such as vegetation filtering, triangulation, hole filling, morphological analysis, change analysis.

7. Results are manually reviewed and revised for consistency.

The above methodology was used to perform the preliminary analysis presented below; a detailed update will be included in future versions of the project methodology.

3.1.1 Overview

This section summarizes changes observed at the sites. In order to gain an understanding of the changes that occur at each site across seasons, and eventually to evaluate the impact of climate change, analysis was performed between each survey epoch rather than from the earliest to the most recent epoch. Each epoch is referred to by the season that occurred between the two

surveys that bounded it (e.g., Winter 2017 represents the change epoch that occurred between the Fall 2016 survey and the Spring 2017 survey). In the analyses in this section, activity rate is defined based on Dunham et al. 2017 as the ratio of cells that have failed versus the total number of cells within a section based on the RAMBO output. Table 3.1 and Figure 3.1 present the annual activity rates observed at each site. Failure depth is defined in Dunham et al. 2017 as the average amount of recession into the sea cliff based on the RAMBO output. Table 3.2 and Figure 3.2 present the average failure depths observed at each site.

Table 3.1: Statistics of Annual Activity Rates (% per year expressed in decimal form) for all Epochs Across each Site.

Statistic	Arch Cape	Silver Point	Spencer Creek
Average	0.195	0.502	0.405
Standard Deviation	0.108	0.412	0.220
RMS	0.217	0.623	0.450

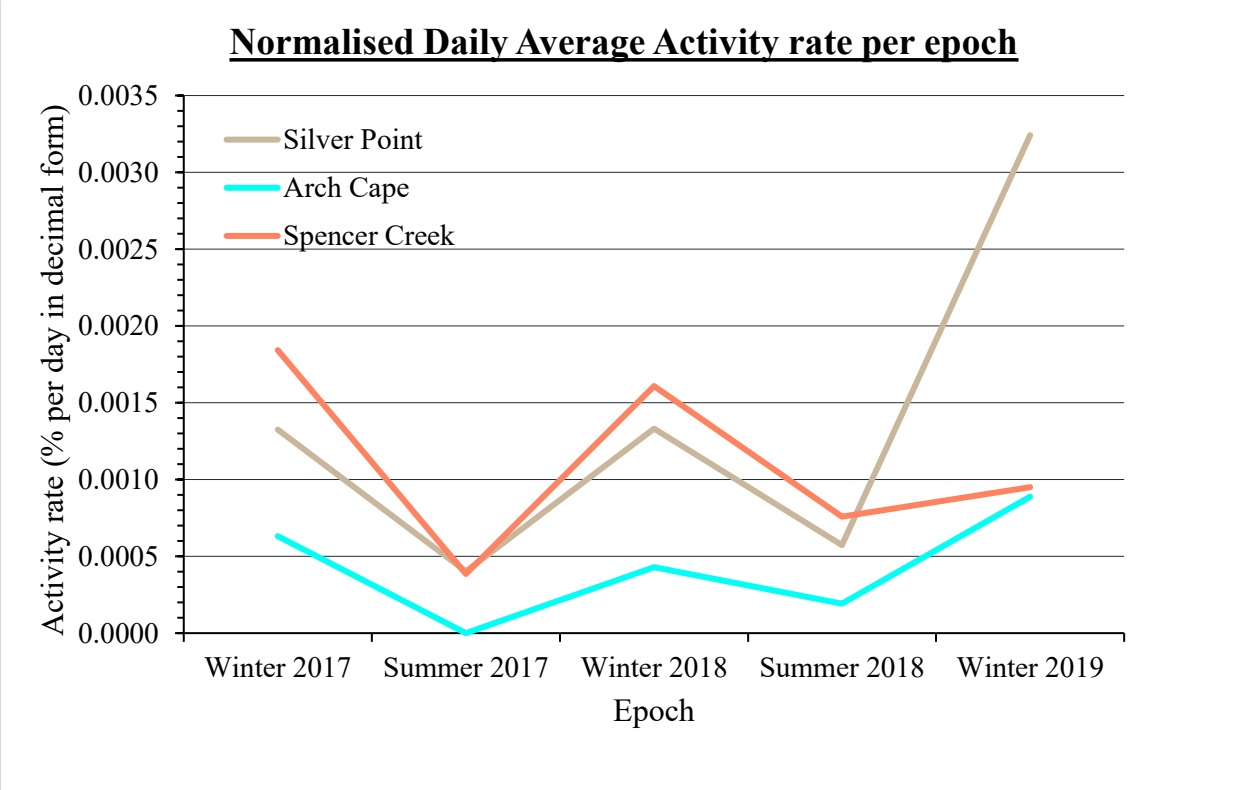

Figure 3.1: Activity rate at each site for each epoch normalized by the number of days between surveys. Note that given the scanner failure in the Spring 2017 survey, a reliable failure depth rate for Arch Cape for Summer 2017 could not be computed.

Table 3.2: Statistics of Annual Failure Depths (m per year) for all Epochs Across each Site.

Statistic	Arch Cape	Silver Point	Spencer Creek
Average	0.410	0.309	0.300
Standard Deviation	0.098	0.078	0.068
RMS	0.419	0.317	0.306

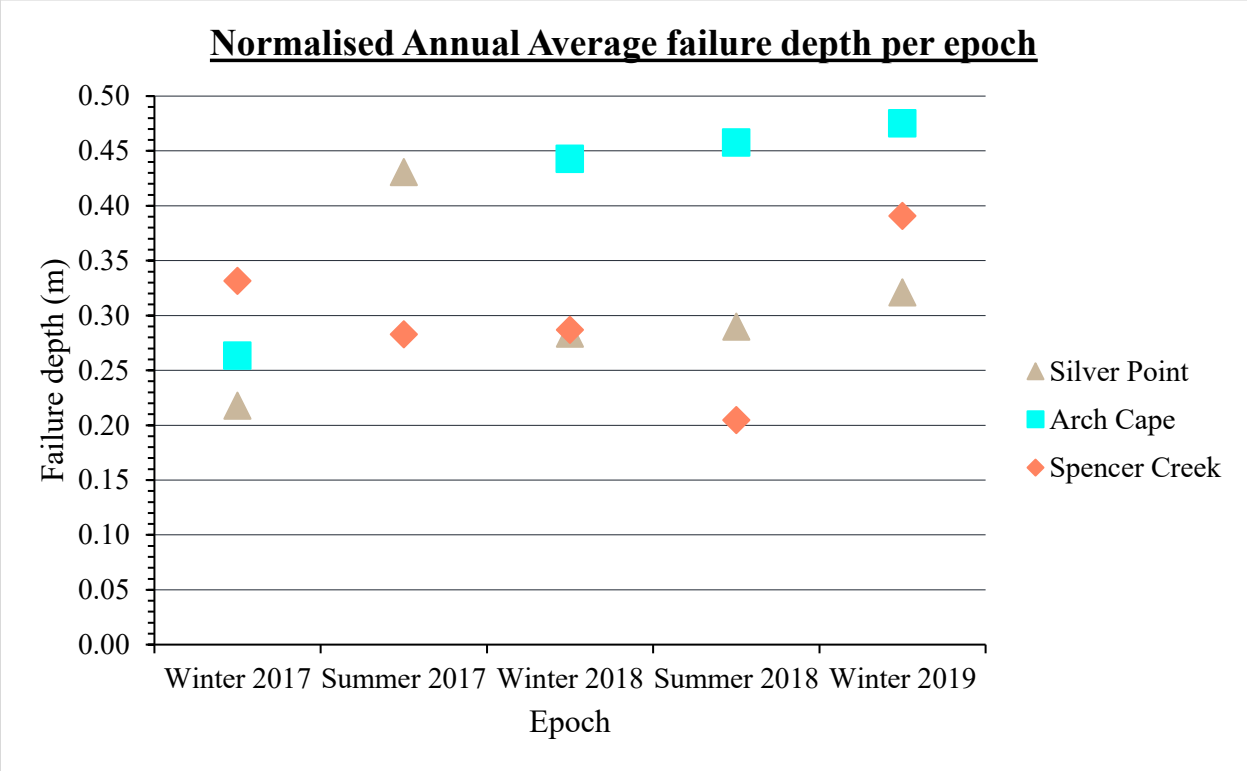

Figure 3.2: Average failure depth for each site per epoch normalized by the number of days between each survey. Note that given the scanner failure in the Spring 2017 survey, a reliable failure depth rate for Arch Cape in Summer 2017 could not be computed.

3.1.2 Arch Cape

Arch Cape has experienced the highest average annual failure depths of the three northern sites in this study (Arch Cape, Silver Point, and Spencer Creek) with an average annual failure depth of 41 cm/yr (Table 3.2). Over the last 2.5 years of this study, Arch Cape has been dominated primarily by rapid erosion at the base of the sea cliff. Figure 3.3 shows the change that occurred at the site between Fall 2016 and Spring 2019 throughout the primary portion of interest (sea cliff immediately south of the tunnel). At the base of the sea cliff the erosion has mostly been between 1m - 2.5 m over the 2.5-year period. Reduced erosion/failures have occurred higher up on the sea cliff at this time, which leads to the relatively low annual average activity rates at this site (Table 3.1); however it is likely that continued higher levels of erosion at the base of the sea cliff may lead to toppling and or sliding failure of the upper slope when analyzed over a longer time period. Table 3.3 summarizes the volume changes and relative failed surface area between

each survey epoch. The most recent epoch (Winter 2019) received the most volume loss -223 m^3 of material across the site. Figure 3.1 and Figure 3.2 show the change in activity rate and average failure depth across each epoch, the annual activity rate varies between 0.07 in Summer 2018 and up to 0.32 in Winter 2019, whilst the annual failure depth varies between 0.26 m in the Winter 2017 and up to 0.48 m in Winter 2019.

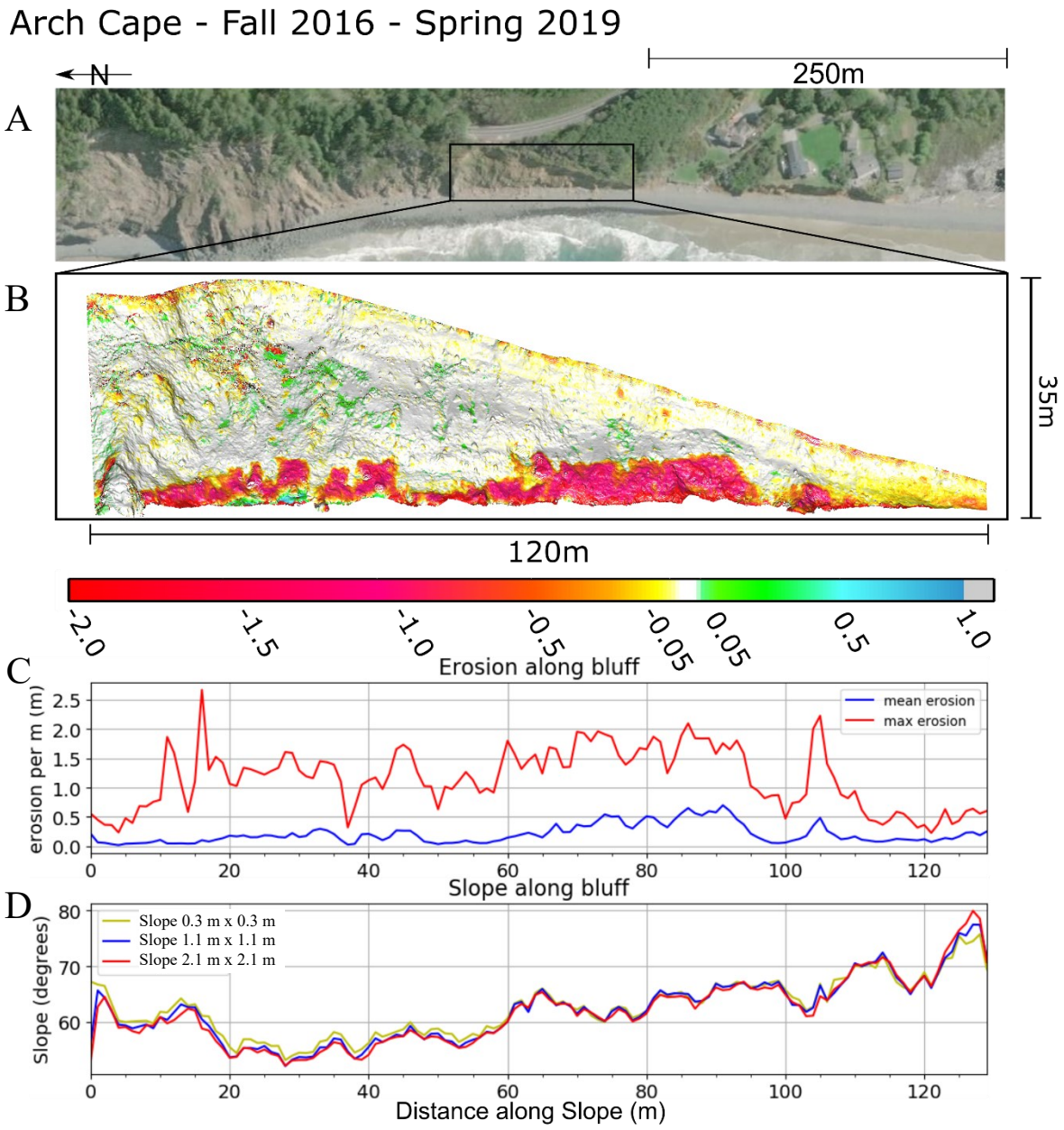

Figure 3.3: Erosion occurring between the start of the project (Fall 2016) and the most recent epoch (Spring 2019) along the main sea cliff at Arch Cape. A) An aerial view of the area of interest. B) Pointcloud displaying change in meters between epochs. C) The mean and max erosion depth that has occurred in 1 m horizontal bins along the sea cliff. D) The mean slope value for several window sizes along 1 m horizontal bins.

Table 3.3: Summary Statistics of Volumetric Change between each Epoch at Arch Cape from Fall 2016 to Spring 2019.

Epoch	Days between survey	Surface area (m^2)	Failed volume (m^3)		Failed surface area (m^3)		Failed volume per area (m^3/m^2)	
			Total	per year	Total	per year	total	per year
Winter 2017	268	4298	-140	-190	2422	3298	-0.021	-0.029
Summer 2017	N/A							
Winter 2018	349	2752	-183	-191	819	857	-0.064	-0.067
Summer 2018	146	4347	-28	-69	922	2304	-0.004	-0.011
Winter 2019	212	4526	-223	-384	2719	4682	-0.043	-0.074

3.1.3 Arizona Inn

Unlike the other four sites, the sea cliff at Arizona Inn is not surveyed bi-annually using terrestrial lidar due to fact that the beach is inaccessible from land when carrying survey equipment. Nevertheless, to date, three UAS SfM/MVS photogrammetric surveys, and one UAS lidar survey have been conducted to provide pointcloud data of the sea cliff. The first UAS SfM/MVS photogrammetric survey occurred in 2016 using the SenseFly Albris UAS system. In order to correctly georeference pointcloud data associated with this system reference targets must be placed and surveyed using GNSS/Total station surveying solutions. Given the inability to access the beach/sea cliff at this site, no targets could be placed at these locations and thus accurately surveying this section of the site was not possible. As of December 2018, OSU acquired a DJI Phantom 4 Pro (P4P) UAS system that is capable of direct georeferencing. The DJI P4P is also capable of recording raw GNSS observations allowing for a PPK (post processed kinematic) solution, enabling an estimate (on the order of several cm's) of the camera origin for each photograph to be calculated, significantly reducing the reliance on targets. However, some ground control targets are still recommended for verification and quality control.

Figure 3.4 shows a pointcloud of the sea cliff in Arizona generated from photographs acquired with the DJI P4P during the Spring 2019 survey. This UAS SfM/MVS photogrammetric data is now expected to be collected every 6 months during the bi-annual field surveys and should allow for change metrics (including change deltas, volume loss, and failed area) to be calculated as it is for the sea cliffs at the other sites. In addition, UAS lidar data was collected in Spring 2019 at this site and will serve as a strong baseline for future airborne surveys. At Arizona Inn, TLS surveys have taken place along the road, as well as on the main body of the landslide above the road including the assumed headscarp as shown in Figure 2.2.

In order to perform preliminary analysis and monitor the change that has occurred at the Arizona Inn site several assumed stationary features (telephone poles, reflectors, guard rails, structures

etc.) were extracted from the pointcloud and the distance or offset between surveys was measured and plotted on the map in order to display the movement vectors (Figure 3.5). The average displacement over the 2.68-year time period was 30 cm (11 cm per year) with a max displacement of 71 cm (27 cm in a year). In general, displacements were higher in the southern portion of the landslide, as well as closer to the sea cliff (south-west section of the site). These values line up with field observations where repaving of the road is seemingly performed on a more frequent basis in the southern part of the landslide. The higher movement activity closer to the sea cliff may be induced by the high level of erosion expected at this site. This higher erosion activity has resulted in the generation of smaller progressive landslides within the main landslide body such as the one shown in Figure 3.6, which can be seen at the top of the sea cliff.

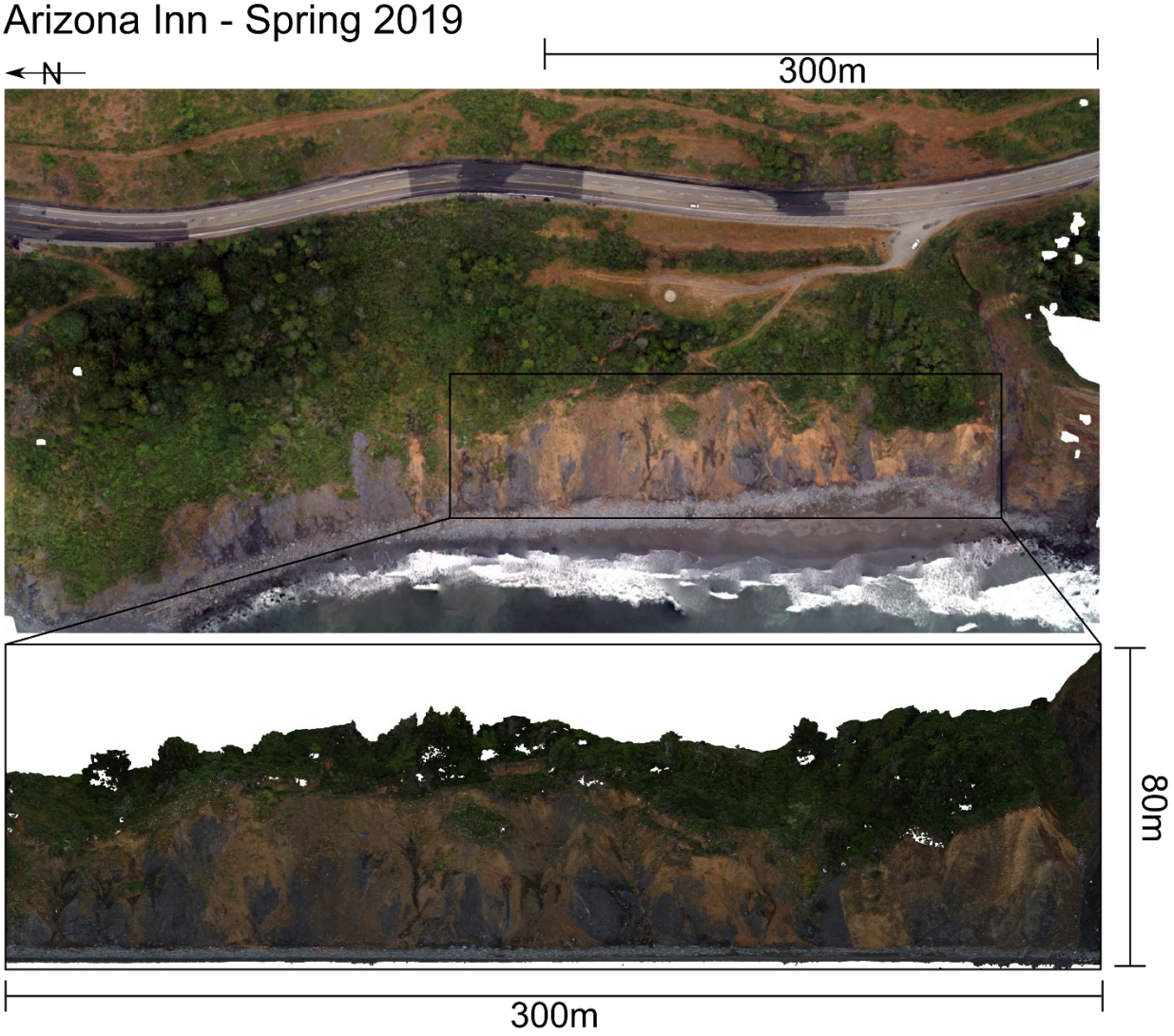

Figure 3.4: UAS SfM/MVS photogrammetric data collected in Spring 2019 on June 24, 2019, using the DJI P4P. The top image shows orthomosaic of the southern portion of the site, while the bottom image shows the generated pointcloud of the sea cliff.

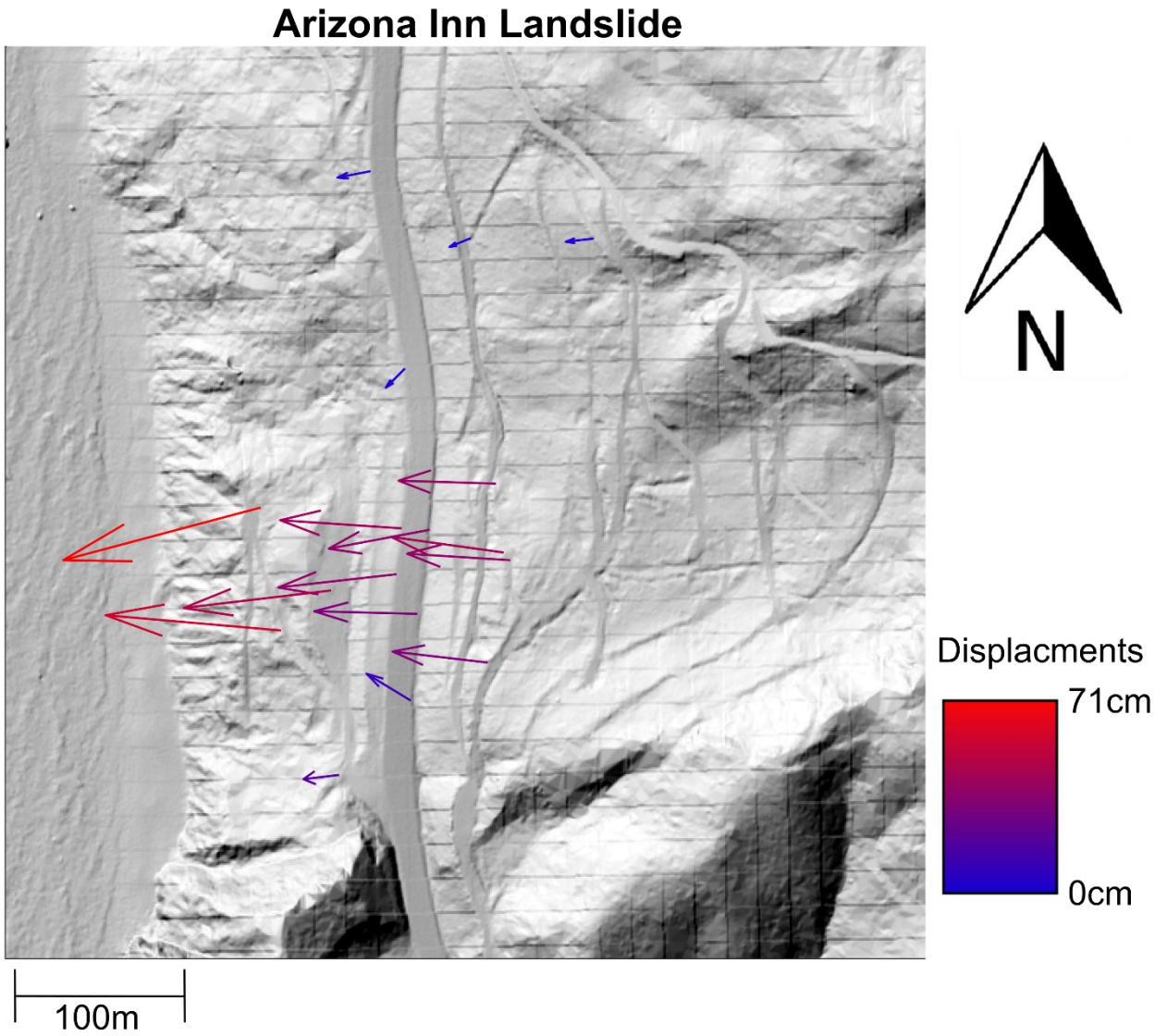

Figure 3.5: Exaggerated (x100) displacement vectors estimated from comparison of TLS pointclouds from October 19, 2016 to June 24, 2019 (978 days, 2.68 years).

Figure 3.6: Development of a headscarp of a smaller progressive landslide within the main landslide body at Arizona Inn directly above the sea cliff from February 2017 (A) to March 2019 (D).

3.1.4 Hooskanaden

At a scale much faster than the other sites in this project, the sea cliff at Hooskanaden advances towards the ocean at a rapid rate as it is directly contained within the body of the landslide. Change analysis methods (such as those used at Arch Cape, Silver Point, and Spencer Creek) show a net accretion to have taken place across parts of the sea cliff (Figure 3.7). The sea cliff has accreted forward due to the movement/sediment transfer provided by the landslide and thus the coastal bluff is situated within/at the toe of the Hooskanaden landslide. Figure 3.7 also shows more accretion occurring at the south end of the bluff (right hand side of figure). These observations were also further confirmed during the February 2019 landslide event where the beach was uplifted an uneven amount laterally with more uplift occurring in the southern portion of the beach (Figure 3.8).

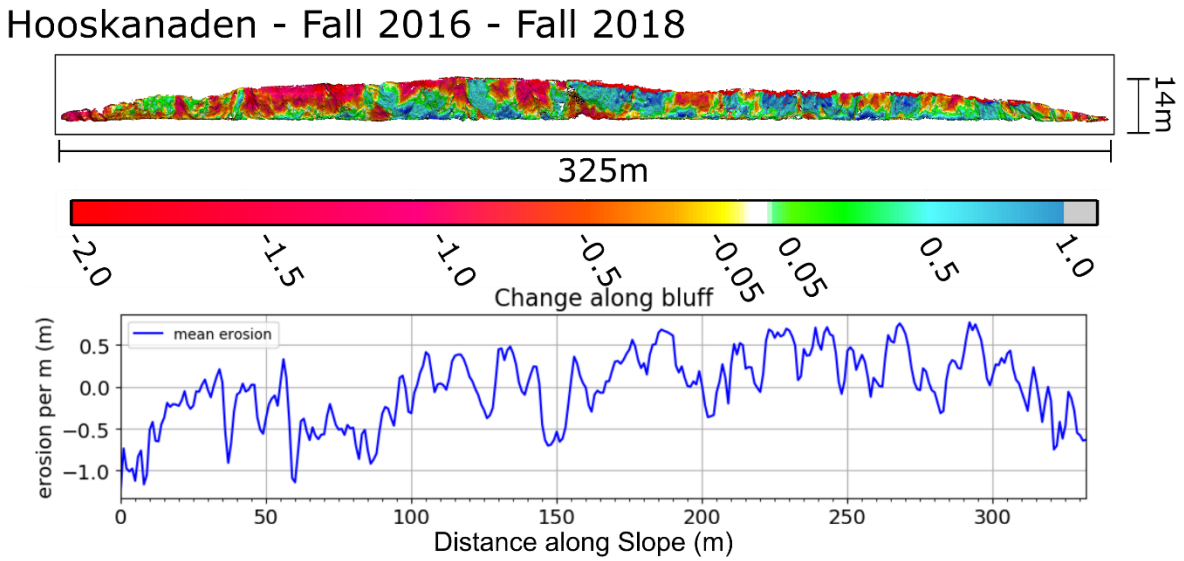

Figure 3.7: Change in the bluff at Hooskanaden from Fall 2016 to Fall 2018 derived from TLS pointclouds. Red (negative values) represents erosion while blue (positive values) represents accretion likely due to landslide movement.

In order to quantify/separate the erosion that has taken place at the sea cliff, the movement of the landslide at the sea cliff has to be quantified between the two survey epochs and a transformation/rotation has to be applied (either forward to the baseline survey or reverse to the recent survey) in order to cancel out the effects of landslide movement in the change analysis. In the situation were the sea cliff moved as a rigid body, this would be a fairly straightforward task and an approach similar to Olsen et al. 2012 could be used where trees along the top of the cliff can be used as reference markers to estimate the amount of landslide movement. However, in the case of Hooskanaden the movement along the sea cliff varies significantly laterally and as the landslides moves almost like a semi-rigid earthflow. This is most easily observed in Figure 3.8, which shows the significant lateral variability in uplift proceeding the recent landslide event at Hooskanaden. To overcome this challenge, more research/work needs to be completed in this area in order to create an easily repeatable method of removing landslide movement prior to the change detection analysis being performed.

Further analysis specific to the February 2019 landslide event at Hooskanaden is discussed in Section 3.2.

Figure 3.8: Photograph of portion of the sea cliff at Hooskanaden taken from a UAS on March 3, 2019, during the Hooskanaden landslide event. The photograph shows uneven uplift of beach to create secondary sea cliff, where the right (south) of image has been uplifted significantly more than the left (north) and thus the non-rigid movement of the landslide body.

3.1.5 Silver Point

Silver Point has experienced the lowest average annual activity rate of the three northern sites in this study (Arch Cape, Silver Point, and Spencer Creek) with an average annual activity rate of 20% (Table 3.1). Over the last 2.5 years of this study, Silver Point has experienced laterally consistent erosion at the base of the sea cliff, as well as laterally spaced larger failures higher up on the sea cliff on the portion of interest (west of the two pullouts) as shown in Figure 3.9. The mode of these failures varies laterally with failures on the sandstone sea cliff on the southern portion of the site being primarily toppling failures due to undercutting, while failures in the northern portion of the site are primarily sliding failures. This may be due to the difference in geology, given the harder interbedded sandstone in the southern portion of the site and the loosely packed soil in the northern portion of the site. Table 3.4 summarizes the volume changes and relative failed surface area between each survey epoch. The most recent epoch (Winter 2019) received the most volume loss -653 m^3 of material across the site. Figure 3.1 and Figure

3.2 show the change in activity rate and average failure depth across each epoch, the annual activity rate varies between 0.15 in Summer 2017 and up to 1.00 in Winter 2019, while the annual failure depth varies between 0.22 m in Winter 2017 up to 0.43 m in Summer 2017.

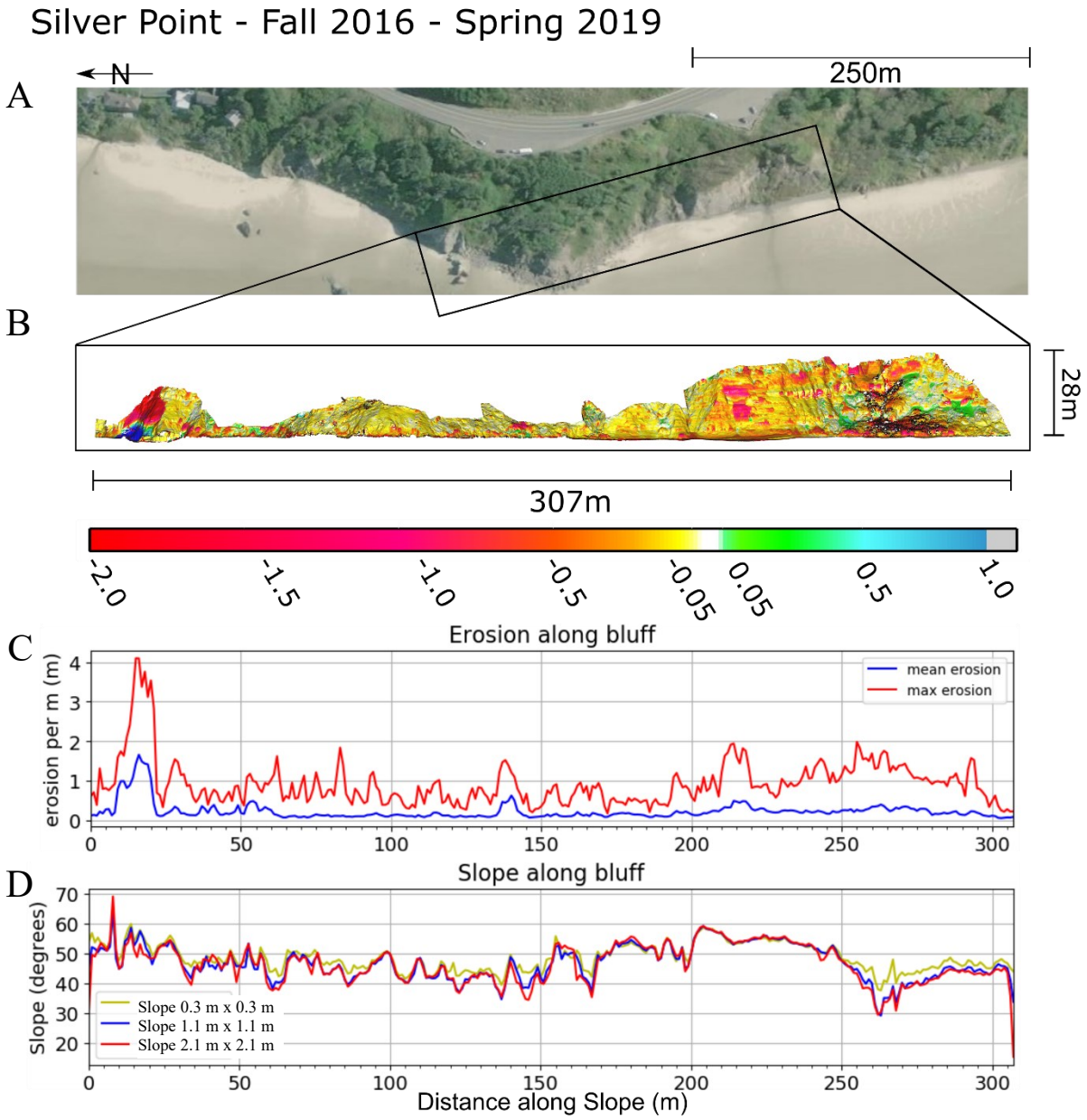

Figure 3.9: Erosion occurring between the start of the project (Fall 2016) and the most recent epoch (Spring 2019) along the main sea cliff at Silver Point. A) An aerial view of the area of interest. B) Pointcloud displaying change in meters between epochs. C) The mean and max erosion that has occurred in 1m horizontal bins along the sea cliff. D). The mean slope value for various window sizes along 1m horizontal bins for different scales.

Table 3.4: Summary Statistics of Volume Change between each Epoch at Silver Point from Fall 2016 to Spring 2019.

Epoch	Days between survey	Surface area (m^2)	Failed volume (m^3)		Failed surface area (m^3)		Failed volume per area (m^3/m^2)	
			Total	per year	Total	per year	Total	per year
Winter 2017	267	6553	-313	-428	3474	4749	-0.041	-0.056
Summer 2017	130	6389	-49	-138	952	2673	-0.006	-0.017
Winter 2018	220	6430	-281	-466	3439	5706	-0.037	-0.061
Summer 2018	145	6495	-84	-211	2607	6562	-0.007	-0.018
Winter 2019	212	6513	-653	-1124	4496	7742	-0.094	-0.161

3.1.6 Spencer Creek

For this analysis, a portion of sea cliff running along HWY 101 south of the Spencer Creek Bridge approximately 600 meters in length was used. Spencer Creek has the 2nd highest activity rate of the three northern sites in this study (Arch Cape, Silver Point, and Spencer Creek) with an average activity rate of 40.5% and a very similar failure depth to Silver Point (30 cm) as shown in Table 3.1 and Table 3.2. Figure 3.10 shows the erosion that has occurred between Fall 2016 and Spring 2019 for a smaller 250 m section of the site centered around the southern SAA. Erosion at this section consists of a mixture of basal erosion of the sea cliff, followed by overhang toppling failures (such as the center of the section). Interestingly, there is some correlation between the average local slope value and the erosion observed. This may be due to over-steepening, resulting in an increase in overhangs/toppling failures. Figure 3.11 shows an example of a toppling failure that occurred at Spencer Creek directly below the southern SAA. The top image shows a photograph of the failure that was captured during the spring 2019 survey while the bottom shows the results of change detection analysis. The boulders fallen from the slope can be seen as accretion (positive change) in the pointcloud. These boulders may act as rip rap and temporarily function as armoring for this portion of the sea cliff. Since this is part of the erosion process it is important to quantify the time taken for this material to be moved/eroded as well as the temporary reduction in erosion at this point of the sea cliff. This will be an important parameter in the development of a retrogressive failure model, and by surveying the sea cliffs for a long period of time an accurate quantitative representation of this natural process can be developed.

Table 3.2 summarizes the volumetric change and relative failed surface area between each survey epoch. At this site, the failed volumes were between 110 m^3 (Summer 2017) and 1137 m^3 (Winter 2017). Figure 3.1 and Figure 3.2 show the changes in activity rate and average failure depth across each epoch, the annual activity rate varies with a low of 0.14 in Summer 2017 up to a high of 0.67 in Winter 2017, while the annual failure depth varies between 0.20m in Summer 2018 and 0.39m in Winter 2019.

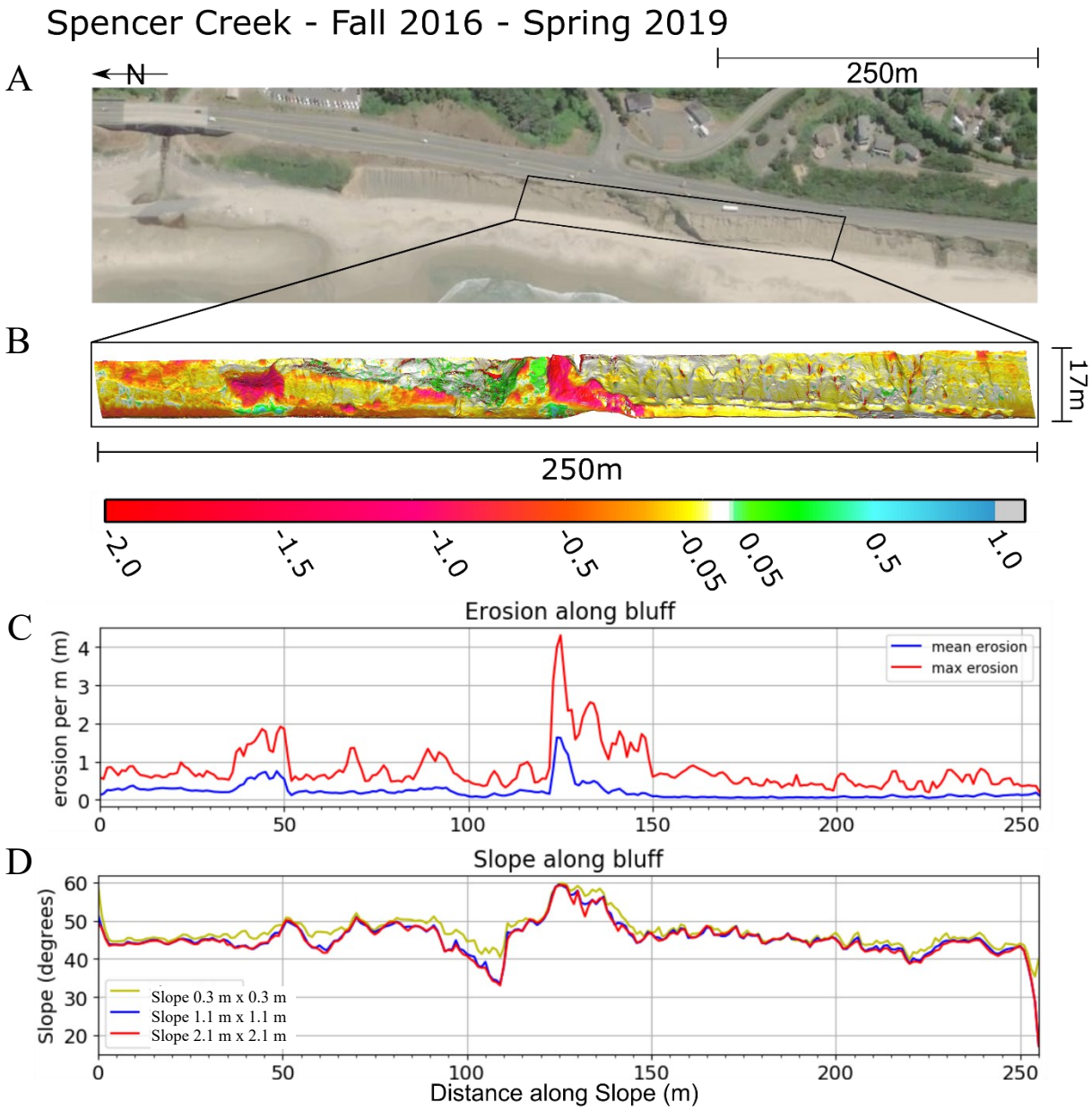

Figure 3.10: Erosion occurring between the start of the project (Fall 2016) and the most recent epoch (Spring 2019) along a 250m section just south of Spencer Creek. A) An aerial view of the area of interest. B) Pointcloud displaying change in meters between epochs. C) The mean and max erosion that has occurred in 1m horizontal bins along the sea cliff. D) The mean slope value for various window sizes along 1m horizontal bins, where 1x1 window size corresponds to 10cm x 10cm, 5x5 corresponds to 50cm x 50cm etc.

Table 3.5: Summary Statistics of Volume Change between each Epoch at Spencer Creek from Fall 2016 to Spring 2019.

Epoch	Days between survey	Surface area (m^2)	Failed volume (m^3)		Failed surface area (m^3)		Failed volume per area (m^3/m^2)	
			Total	per year	Total	per year	Total	per year
Winter 2017	229	12644	-1137	-1813	9696	15454	-0.080	-0.127
Summer 2017	143	12571	-110	-280	2783	7102	-0.006	-0.014
Winter 2018	210	12791	-809	-1406	9995	17372	-0.051	-0.088
Summer 2018	196	12738	-267	-497	6065	11294	-0.015	-0.027
Winter 2019	204	12762	-534	-955	5327	9531	-0.038	-0.068

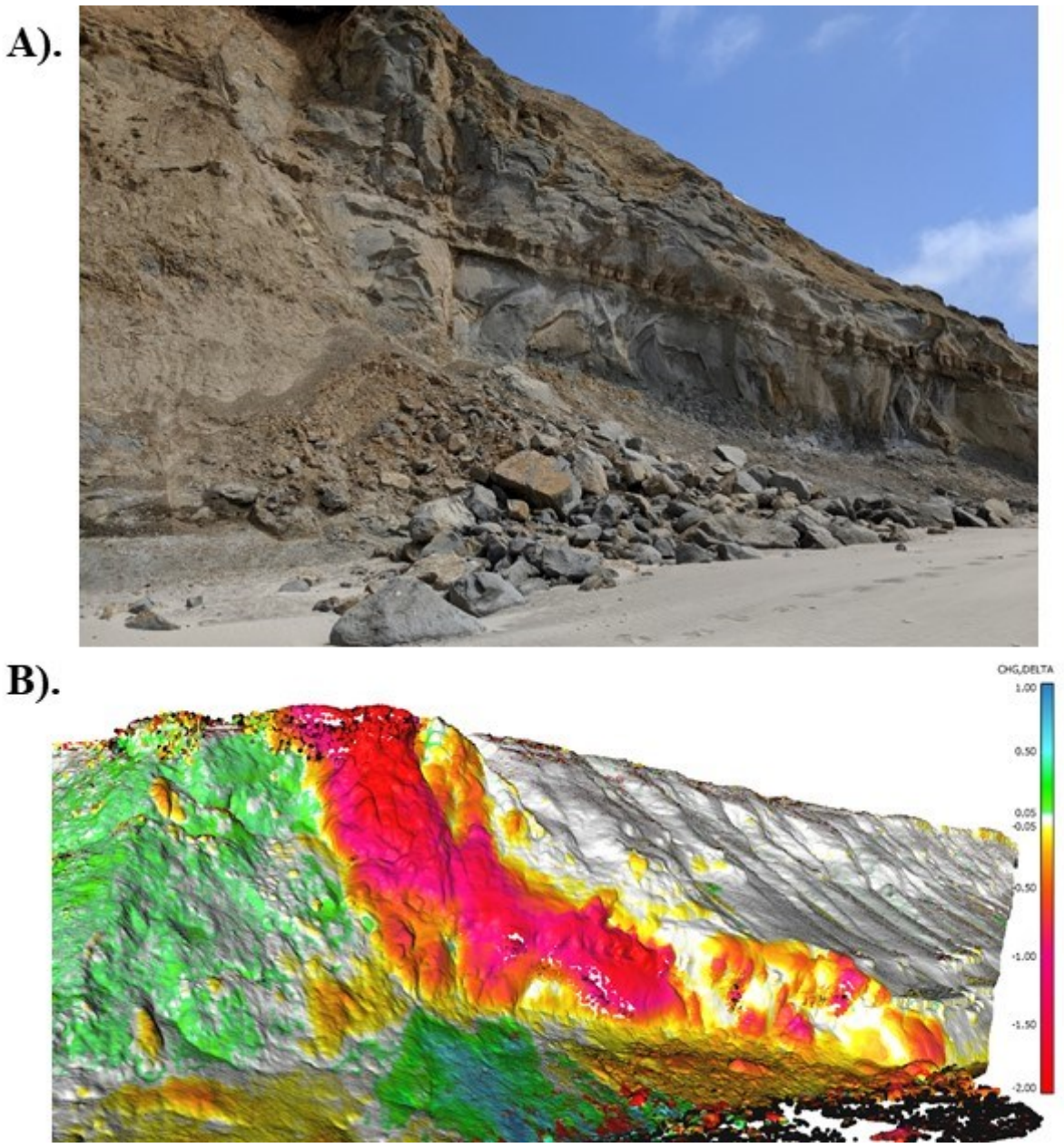

Figure 3.11: Large sea cliff failure that occurred at Beverly beach close to the southern SAA. A). Showing image of debris taken during data collection. B). Pointcloud showing change that occurred between November 8, 2018 and May 31, 2019, red shows erosion and blue/green shows accretion.

3.2 HOOSKANADEN LANDSLIDE EVENT

Hooskanaden demonstrated significant mass movements in early March of 2019 as a result of a period of intense rainfall (more than six inches of precipitation in 24 hours). While the landslide has been historically active with several large movements in the past several decades, this represents the first major event in over 20 years. A comparison of TLS and UAS data enabled digitization of 3D vectors representing the kinematics of the failure. These vectors were created

by selecting similar features (i.e., utility poles, trees, stumps) in Potree visualization (Data available at: http://research.engr.oregonstate.edu/geomatics/projects/OregonCoast/Hooskanaden/Feb2019/lidar/), and represent the epoch between October of 2018 and March of 2019 (Figure 3.12). The vectors of movement highlight that the greatest mass movements occurred in the central part of the earthflow that traverses Highway 101, corresponding to the steepest topography at the site. Movements in the central portion of the earthflow ranged from 15 to 40 meters of 3D displacement, generally oriented in the downslope direction of the topography. More modest movements (2-5 meters) were observed upslope in (1) the major contributing area that nears Carpenterville Highway, and (2) on the northern flanks of the landslide. These significant, but more modest movements are an expression of extension, which is corroborated by numerous tension cracks observed throughout in this portion of the earthflow (Figure 3.13-D). Downslope of the most active portion of the earthflow is a relatively gentle bench, which exhibited moderate displacements, ranging from 5-10 meters. This portion of the earthflow begins at the base of the most active landslide zone and ends the Pacific Ocean. The lower displacements with respect to the central portion of the slide mass are and expression of compression, which is corroborated by notable heave. Heave within the mass was on the order of 3-5 meters near the ocean, most notably observed as a fault gouge that daylighted within the narrow beach at the base of the earthflow (Figure 3.13-A). Superficially, this heave looked similar to a sea cliff, and suggests that the end of the earthflow exists beyond the sea cliff at the base of the landslide. The compression from the upper block likely caused modest subsidence at the head of the lower block (the toe of the central, most active region) and heave at the toe of the lower block. This suggests that the lower block, which primarily consists of landslide deposits, responds to significant activity of the most active region.

After the main failure, the landslide continued to move/flow at rates of approximately 1 ft/ hr. Several UAS photogrammetric surveys were completed during this time. A particle image velocimetry (PIV) analysis (Figure 3.14) was completed to evaluate the horizontal movement occurring at the site. Two composite orthophotos from surveys approximately 24 hours apart on March 2nd and 3rd were compared. From this analysis compression is observed near the toe of the slide where the horizontal displacement vectors become shorter and shorter. Additionally, it appears to consist of two distinct flows between the northern and southern portion of the slide. Example detail images of the orthophoto collected on March 3rd survey are shown in Figure 3.15.

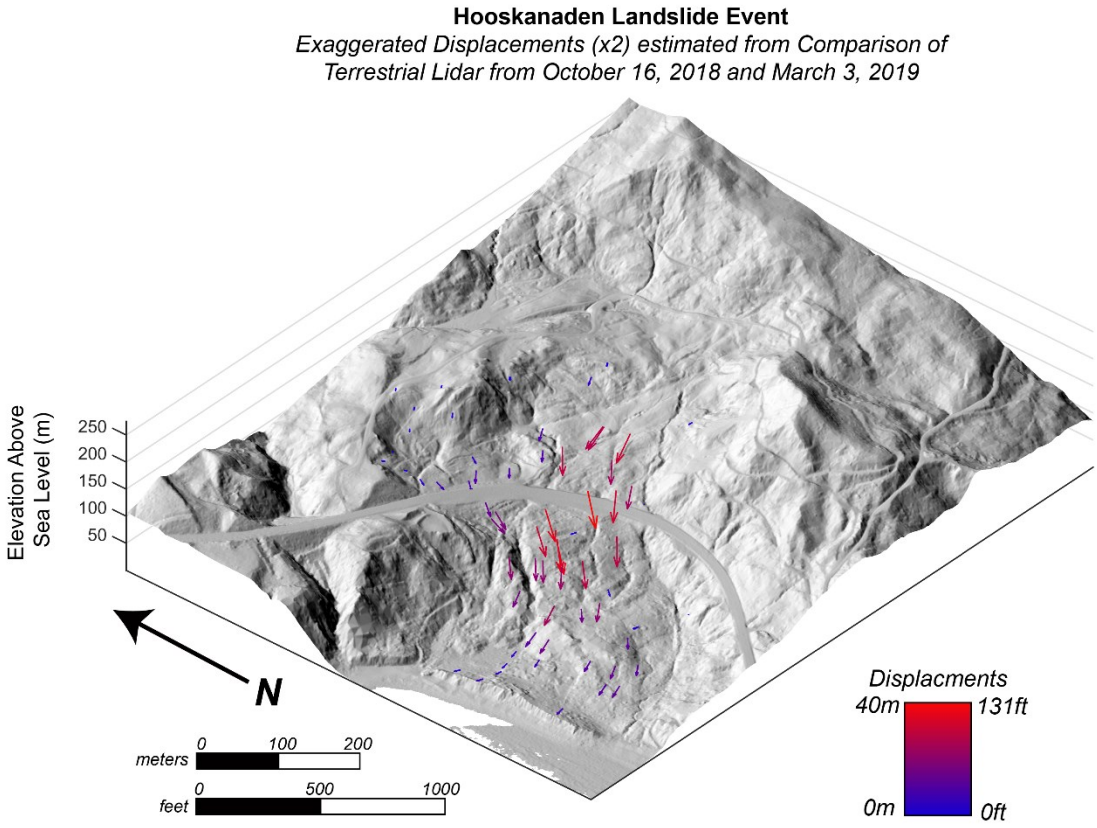

Figure 3.12: Showing 3D movement vectors across the Hooskanaden landslide. These vectors were created by extracting similar features (i.e. utility poles, trees, stumps) from TLS derived pointclouds, representing a time period between October 16, 2018 and March 3, 2019.

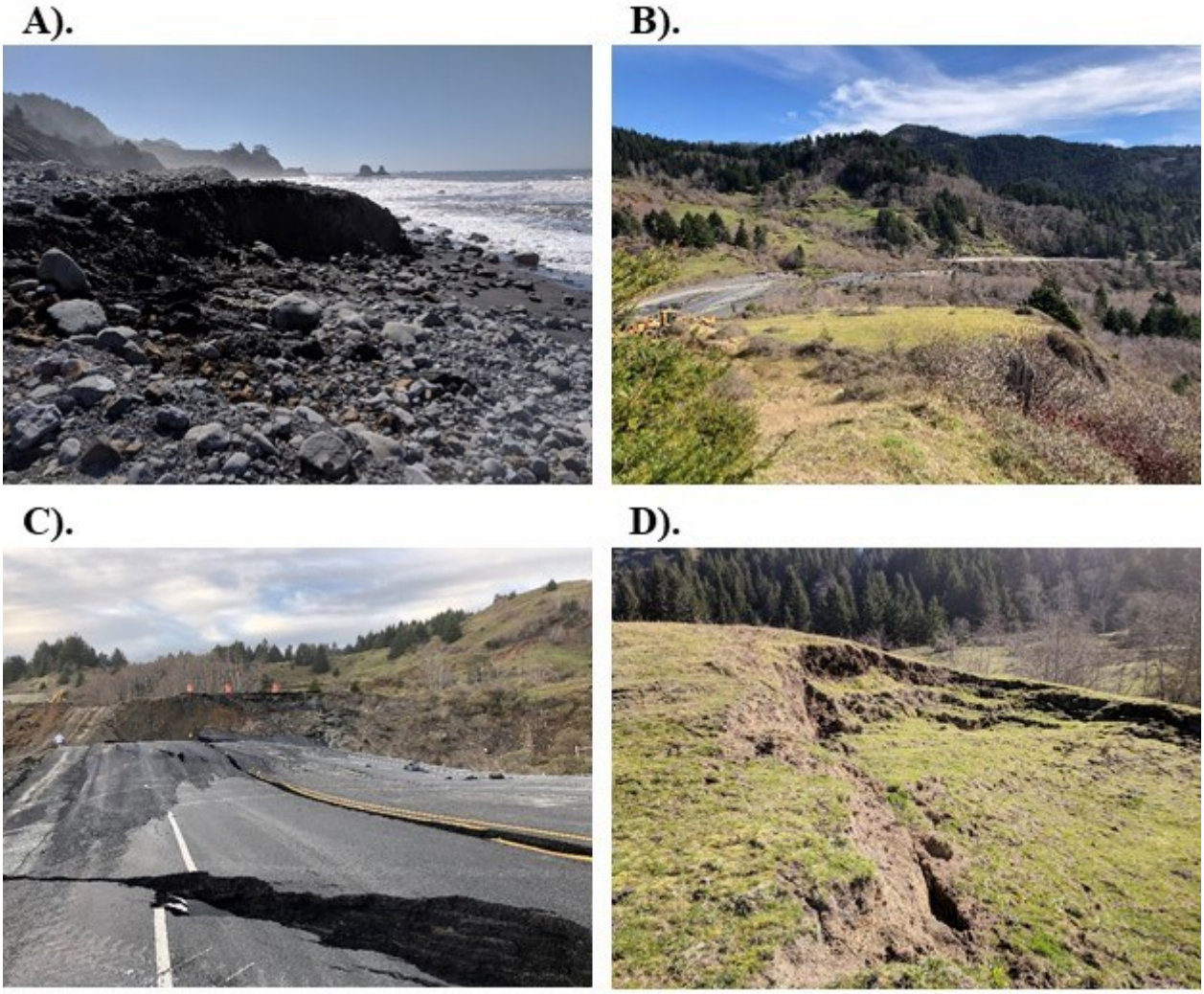

Figure 3.13: Photographs taken in early March 2019 shortly after the Hooskanaden landslide event. A). Shows uplift of the beach at the toe of the landslide. B). Shows an overview of the damage caused to HWY 101. C). Shows close up damage caused to the road by the landslide. D). Shows an example tension crack/scarp from the upper portion of the landslide (above the road).

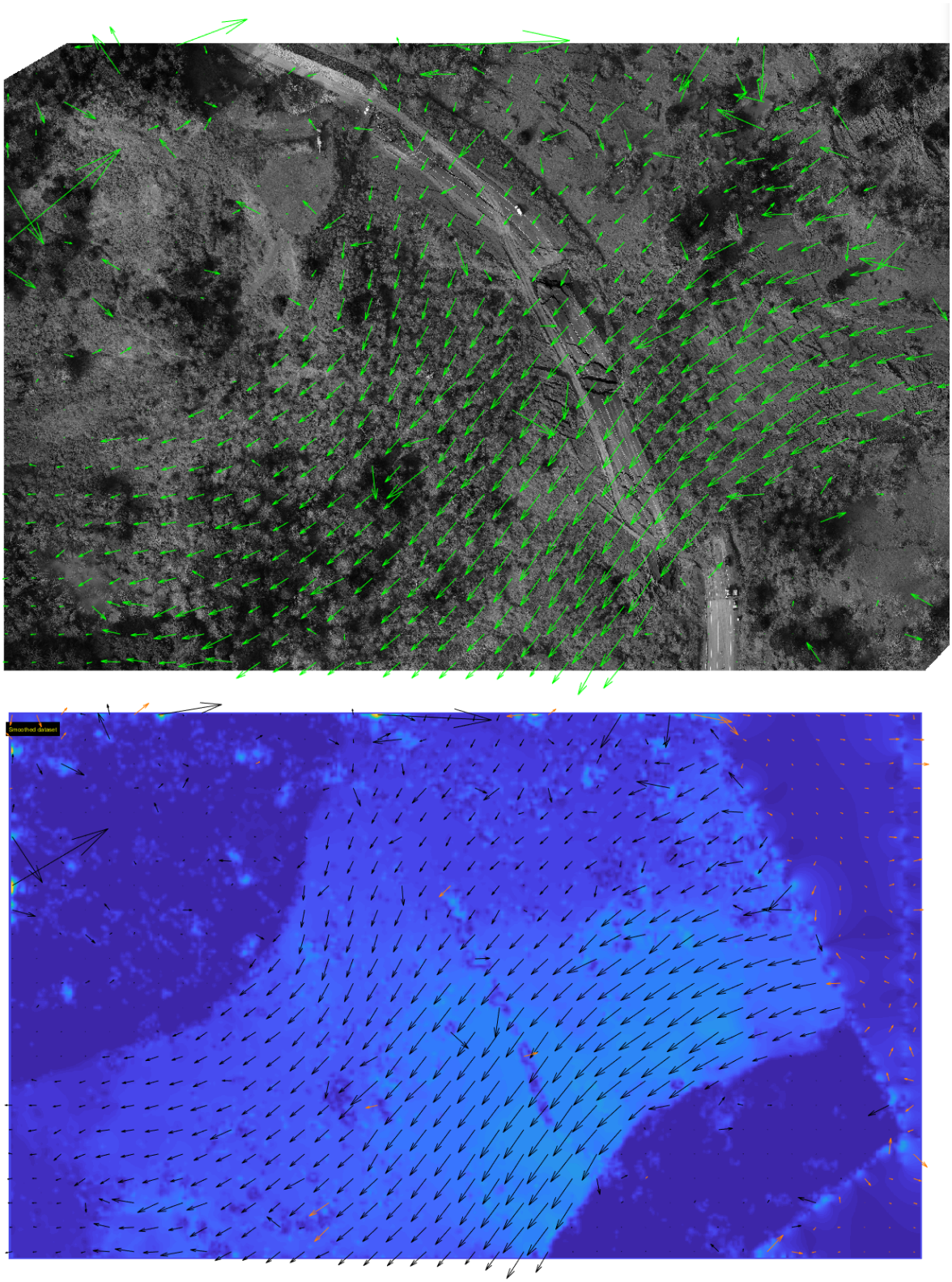

Figure 3.14: Particle image velocimetry (PIV) analysis of the two UAS photogrammetric surveys completed of the slide in late February 2019. The surveys were approximately 1 day apart when the landslide was moving at a rate of approximately 1 ft per hour.

Figure 3.15: Detailed orthophotos acquired for the site on March 3, 2019. The orthophoto and SfM/MVS derived DSM can be explored at: https://research.engr.oregonstate.edu/geomatics/projects/OregonCoast/Hooskanaden/Feb2019/uas/ortho/

3.3 DATA VISUALIZATION

A web framework for displaying pointcloud data collected as part of the project is currently being developed. This framework will likely be similar to that of the digital-appendix from SPR809 - https://research.engr.oregonstate.edu/geomatics/projects/rockfall/spr-809/digital-appendix/ (Figure 3.16). Given this project is set to contain significantly more datasets (7 years of bi-annual scans), more care will be given to setting up easily repeatable and updateable html formatting. This will likely include scripts for generating/updating html files as more survey epochs become available to ensure the website is easily updatable in the future. The authors will update ODOT as this site begins to roll out.

In addition to the above, a web framework for visualizing and manipulating the inclinometer data along with the point cloud in a potree view was developed (Figure 3.17). This interface allows users to: view the displacement over time, exaggerate the displacement (both horizontally and vertically) for easier viewing, change the radius of the inclinometer, view a color-coded legend of the soil layers, and animate the displacing inclinometer through time. This can be viewed for the Hooskanaden site at the following web address: https://research.engr.oregonstate.edu/geomatics/projects/oregon-coast/spr807/hooskanaden/inclinometer-view.html

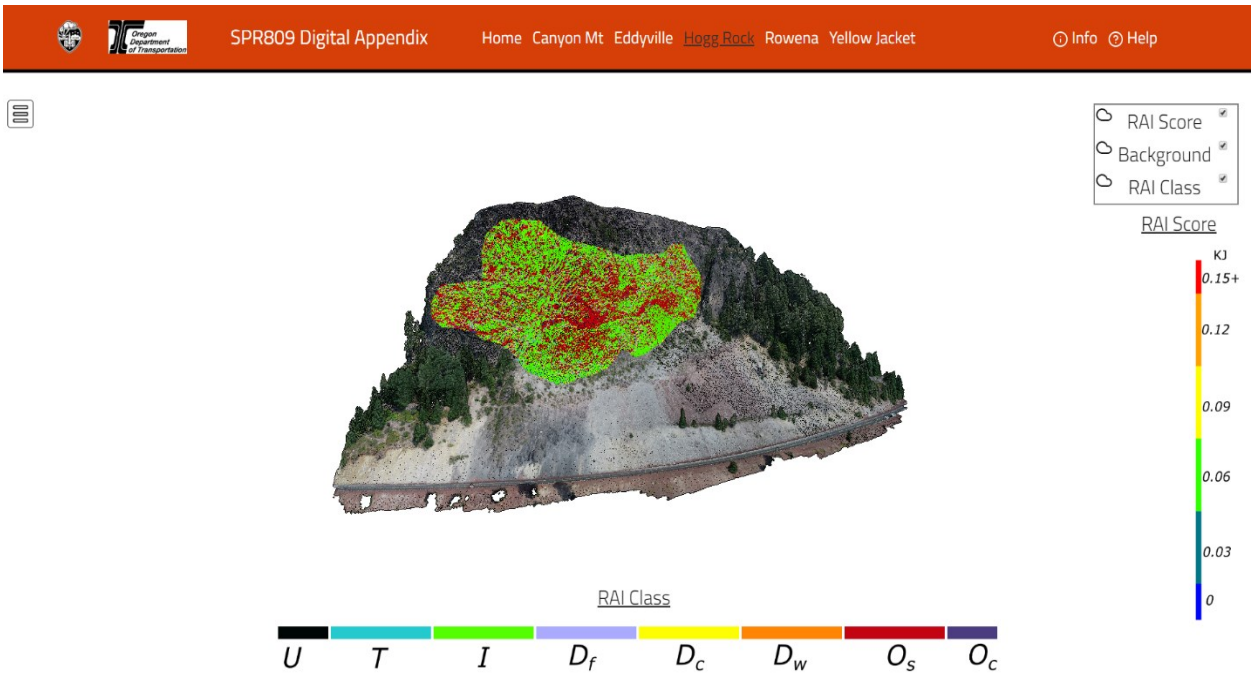

Figure 3.16: Interface of the digital appendix developed during the ODOT SPR809 project.

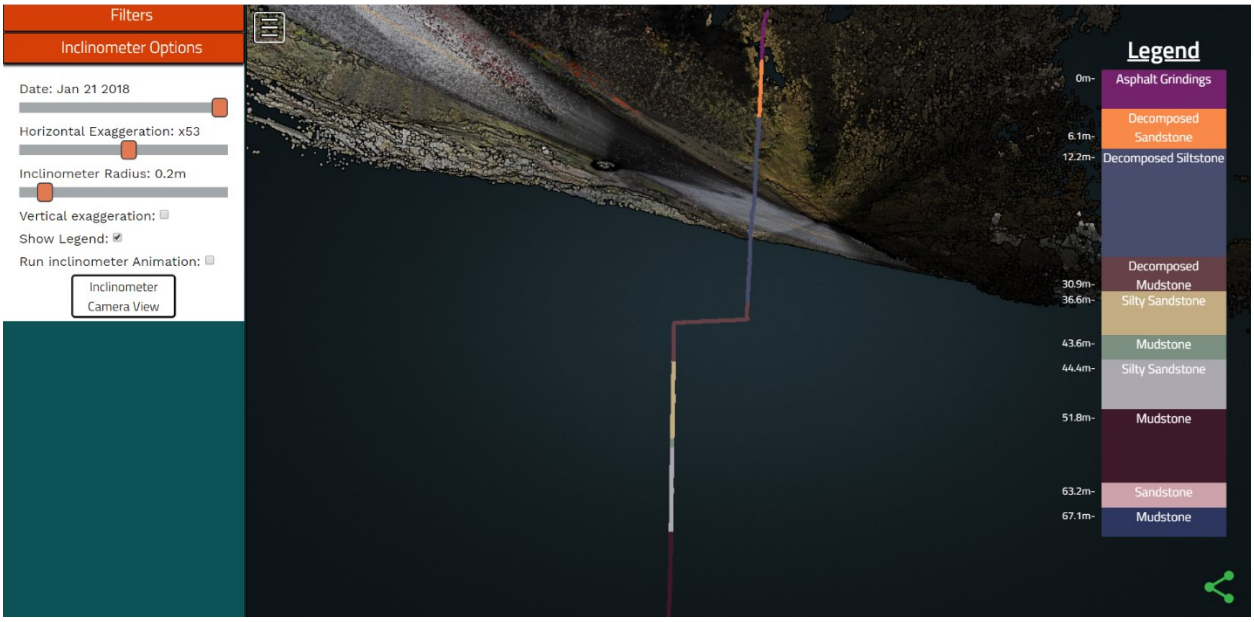

Figure 3.17: Interface of interactive inclinometer within a potree view. Along with options to manipulate the inclinometer (on the left) and a scale bar on the right.

3.4 FIELD INSTUMENTATION DATA ANALYSIS

This section describes the current analysis results from the instrumentation installed at the sites.

3.4.1 Hooskanaden

Hooskanaden has been the most active landslide of the six monitored sites. An inclinometer was installed in November 2017, and soon thereafter sheared along with piezometers by January of 2018 with over 150 mm of displacement (Figure 3.18). The shear plane was measured at 35 meters, and the shear profile was used by ODOT R3 engineers after the significant movement that occurred in 2019. No borings or monitoring had been installed in the landslide to date, thus this data was invaluable for repair efforts of HWY101 after failure. At the time of installation, Hooskanaden exhibited a relatively constant velocity of 3 mm/day. This is commensurate with yearly velocities of 1-2 meters per year (under progressive, but not catastrophic failure conditions). Piezometric levels did not change significantly after the grout within the borehole had set, but are suggestive of elevated pore pressures that are greater than hydrostatic levels (i.e., 55m of head as compared to 35m of depth). The short lifespan of ground instruments at Hooskanaden has prompted further surface monitoring, including two flights of UAS lidar and installation of a series of GNSS rovers throughout the slide mass (planned for upcoming year – See Section 2.5).

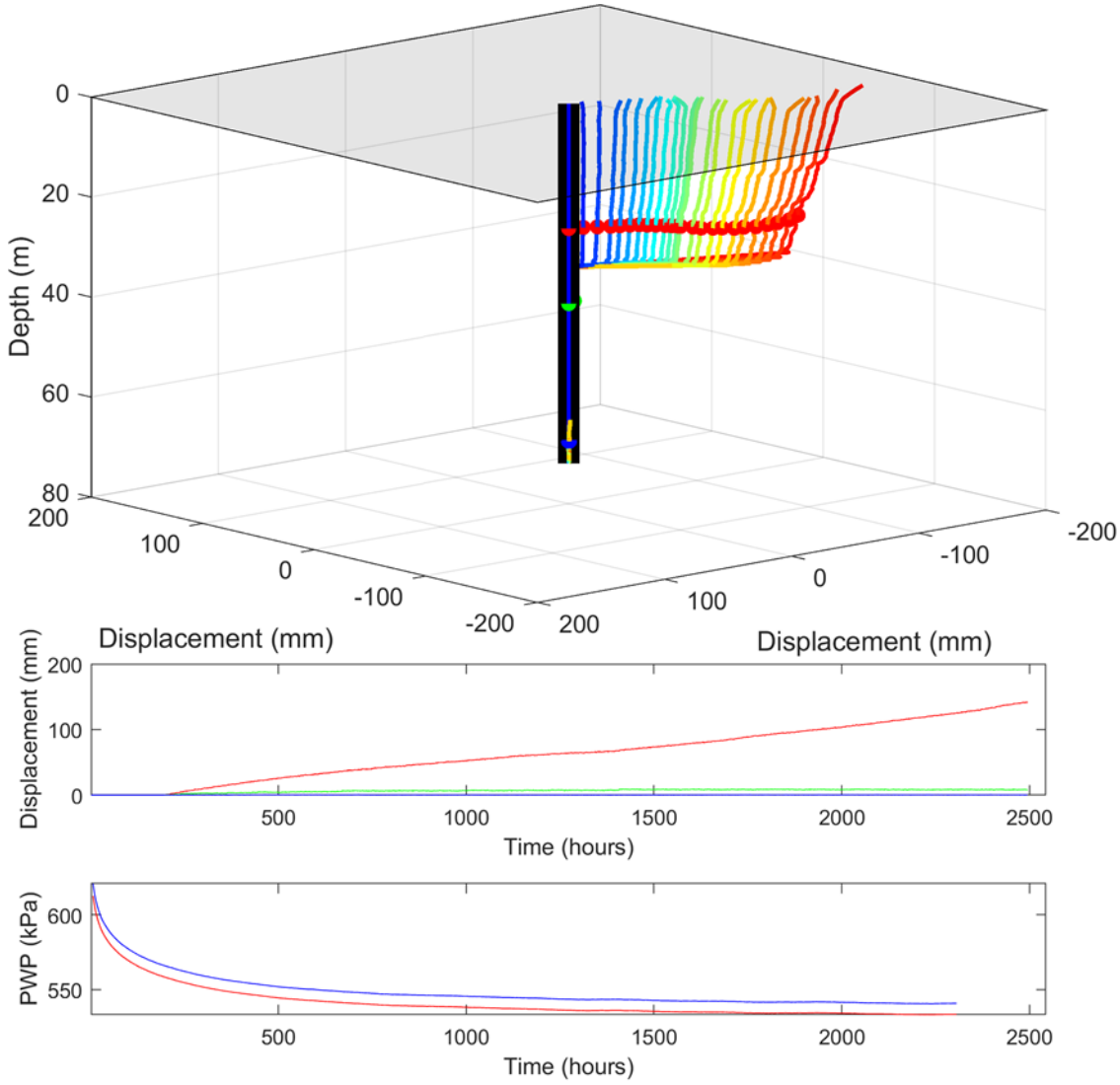

Figure 3.18: Displacements, pore pressures and inclinometer profile from Hooskanaden monitoring site.

3.4.2 Arizona Inn

Arizona Inn has been the second most active landslide of the six monitored sites. It has showed progressive movements since the installation of inclinometers and piezometers. A large seacliff collapse at the toe has been observed since installation and has progressed significantly. During the winter of 2019, there was significant rainfall, resulting in the onset of significant acceleration (almost 10mm in an hour, Figure 3.19 and Figure 3.20). After an early march storm that caused Hooskanaden to fail, the inclinometer system at Arizona Inn also failed. The data on landslide movements and depth of the shear zone was transferred to ODOT Region 3 for use in potential planning for mitigation in the coming biennium, a direct transfer of relevant data. Interestingly,

after movement, piezometric levels dropped in the landslide, owing to significant movement of the lower seacliff collapse. The coupled real-time monitoring of groundwater and a shear profile shown below exhibits the utility of such a coupled system.

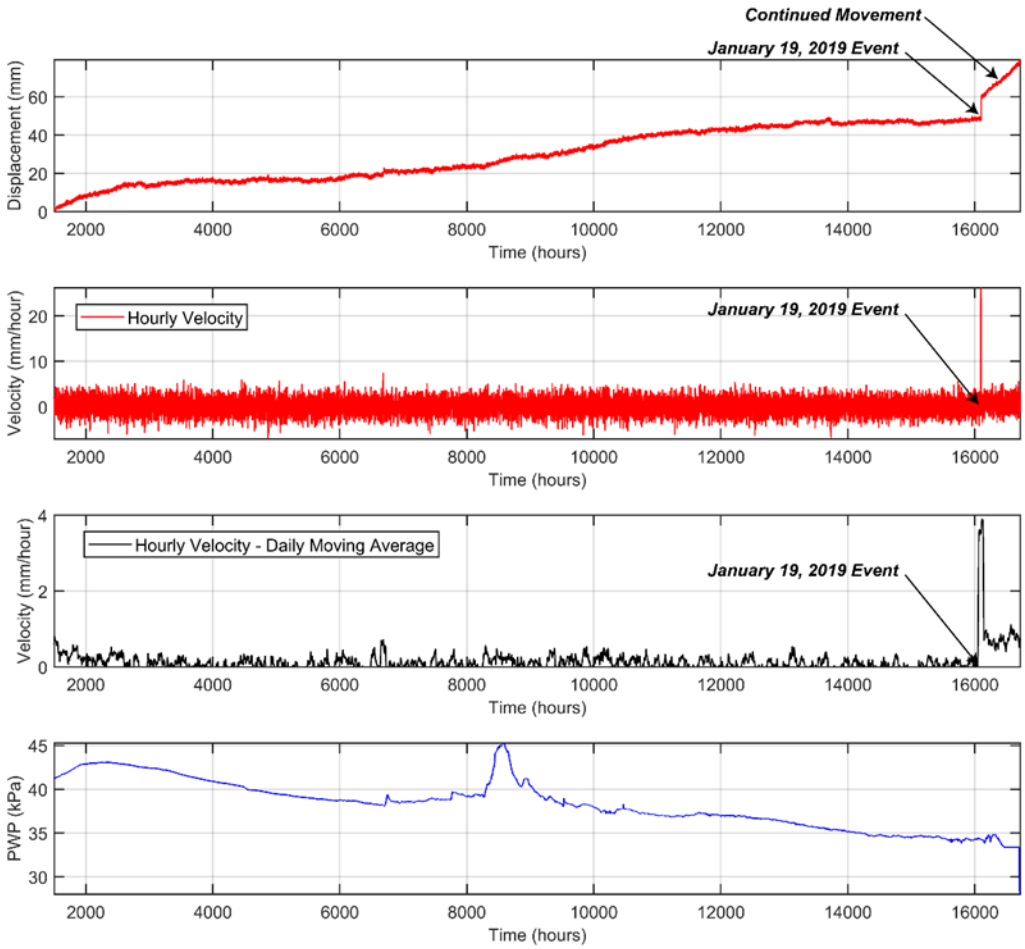

Figure 3.19: Monitored landslide velocities and pore water pressures in the Arizona Inn landslide.

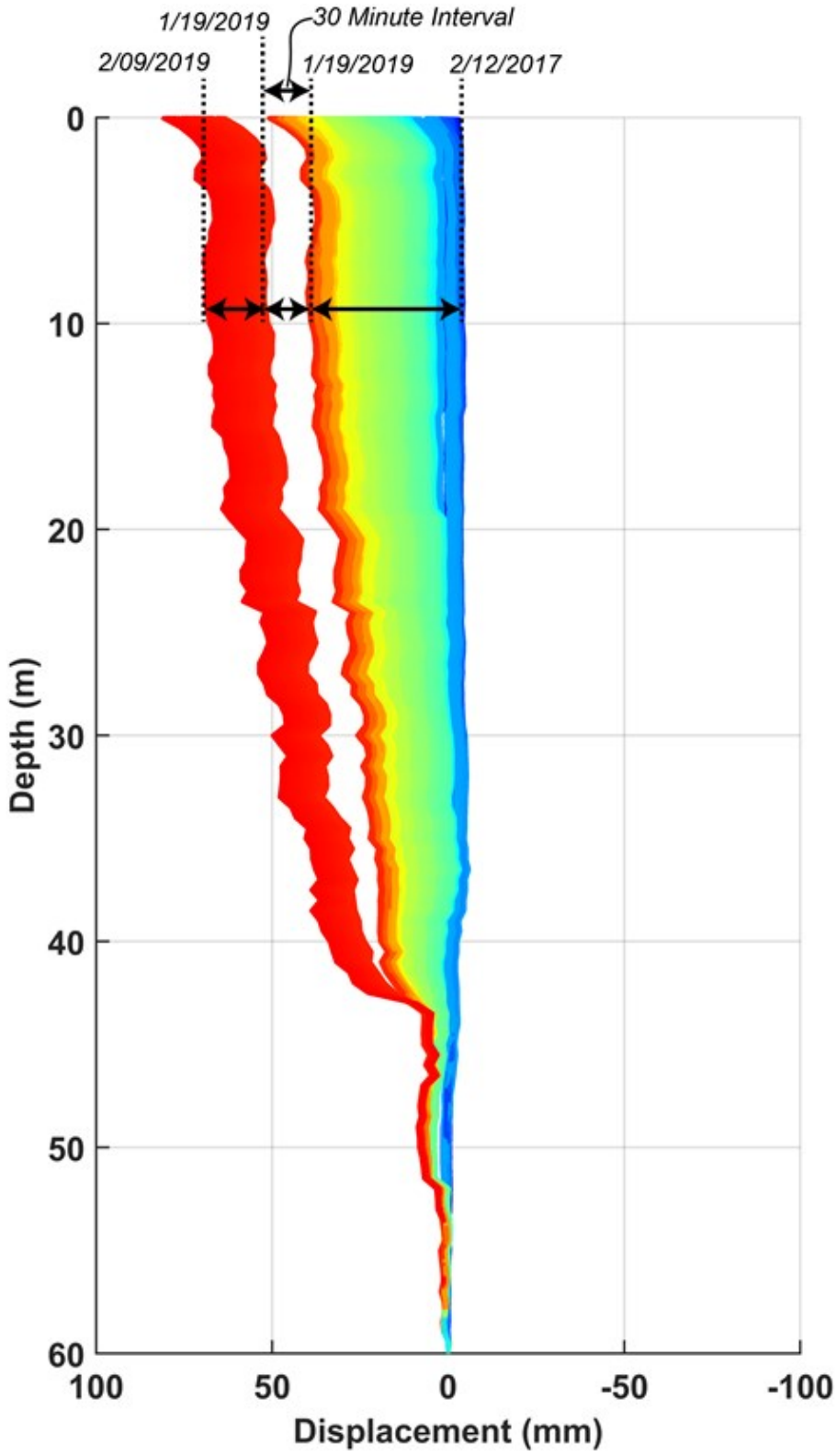

Figure 3.20: Monitored shear profile at the Arizona Inn landslide.

3.4.3 Arch Cape

Arch Cape has been the third most active failure, with notable topping occurring within the monitored inclinometer system. This corresponds to an expression of extension relating to the slump in front of the boring. Overall extension has been almost 150 mm since installation (Figure 3.21 and Figure 3.22), over 50 mm of which may be attributed to ground movements, suggesting movement of the slope failure on the leeward side towards the ocean. This site is by far the most constrained, where progression of slumps from coastal erosion on the narrow beach below may leave limited right-of-way to enter the tunnel just meters north of the site. Interestingly, the piezometric response of the site aligns well with tidal changes (Figure 3.23), suggesting a level of connectivity between the seacliff and the ocean tides. This may result from voids in the cliff (e.g., sea caves) that were infilled with beach sand and then subsequently closed off by landslide deposits from failure of the upper portion of the slope.

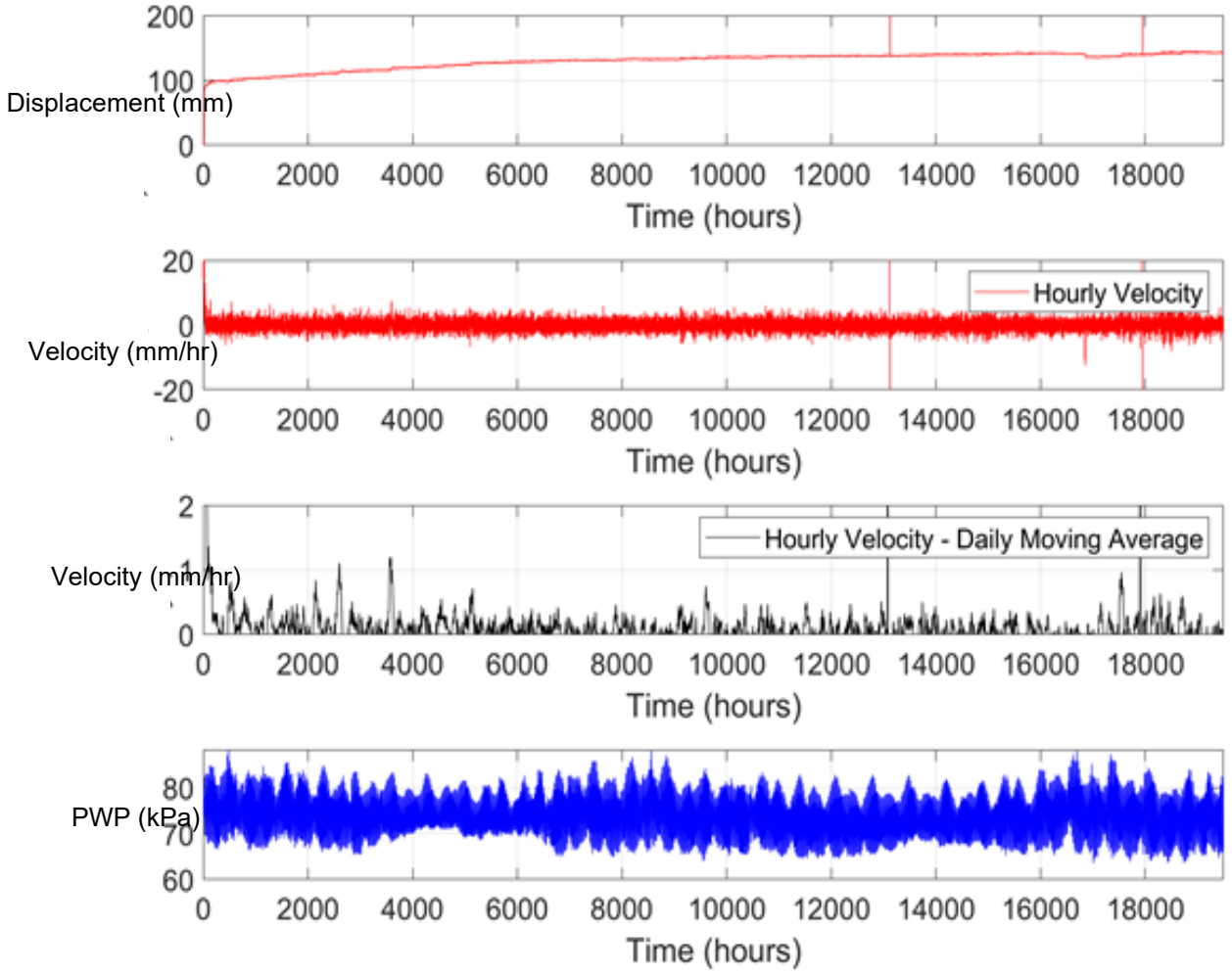

Figure 3.21: Monitored velocities and pore water pressures in the Arch Cape site.

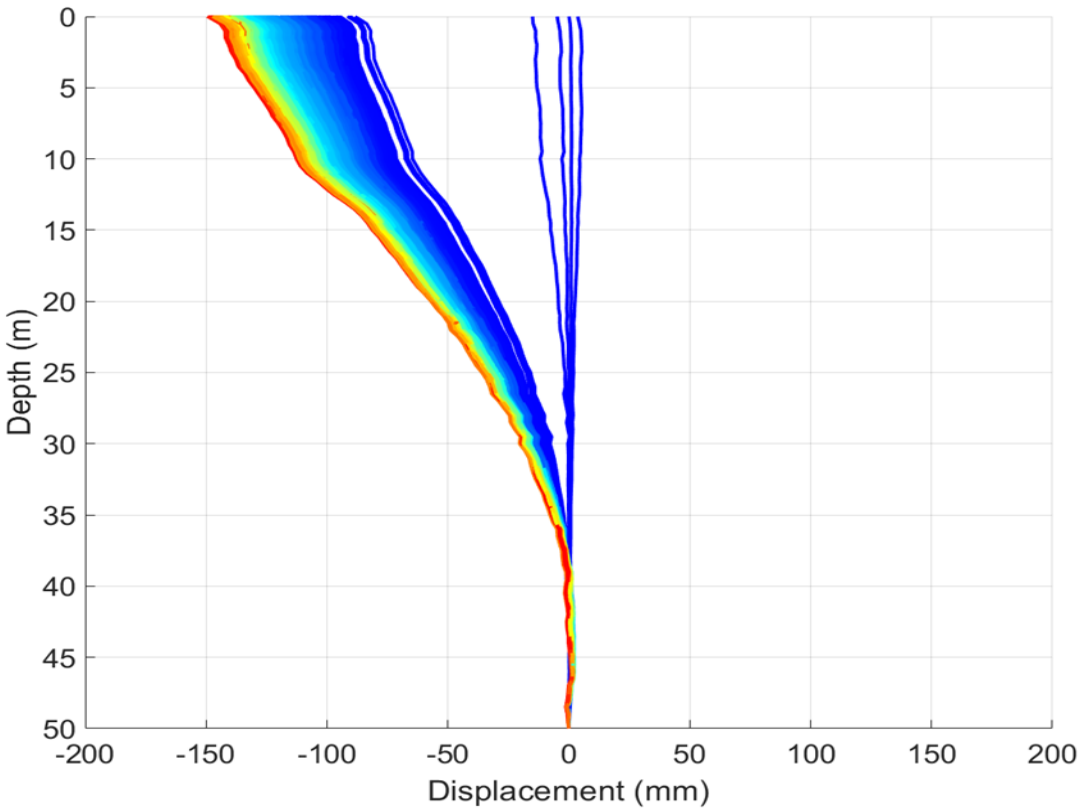

Figure 3.22: Monitored shear profile at the Arch Cape site. The initial discontinuity with time likely reflects settlement of the grout used in installation.

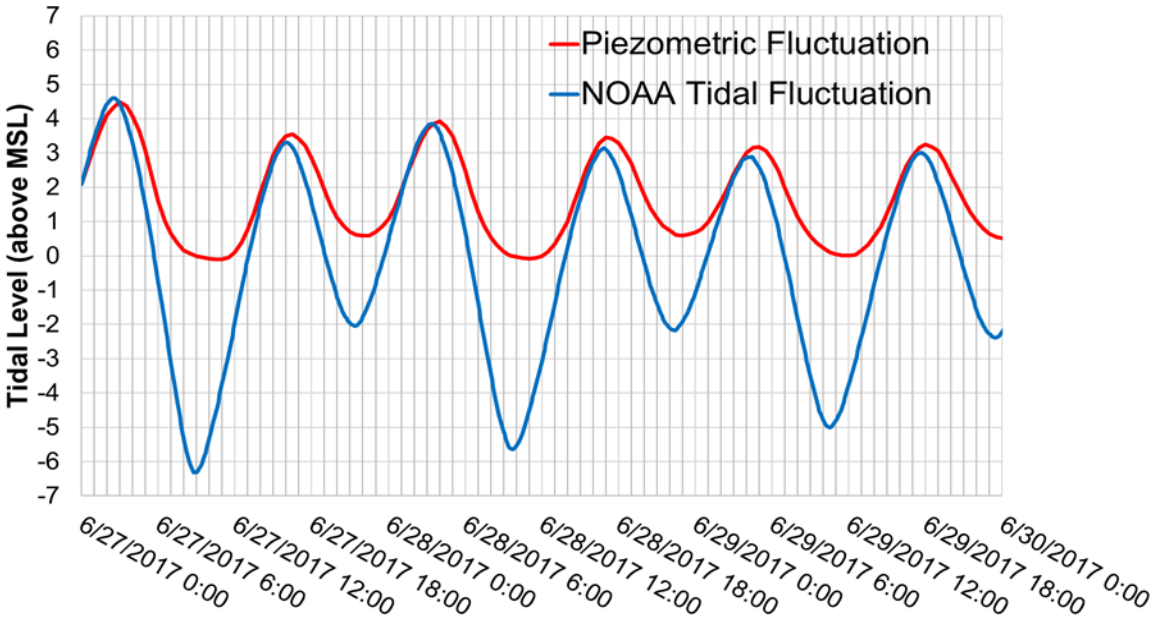

Figure 3.23: Piezometric profile of lower piezometer in comparison to tidal fluctuations.

3.4.4 Spencer Creek South

Spencer Creek South has shown limited deformation since installation of borings in early 2017. It has, however, provided interesting insight into the rate of change in groundwater within the cemented seacliffs that comprise much of Oregon's Central Coast (Figure 3.24). Groundwater levels change rapidly after storm events, gradually dropping to steady state levels after period of modest rainfall. Throughout the wintertime, groundwater levels tend to stay elevated, eventually reaching steady state levels in the relatively dry summer and fall months. This data is directly useful for modelling the role of groundwater in cemented seacliffs along the Oregon Coast.

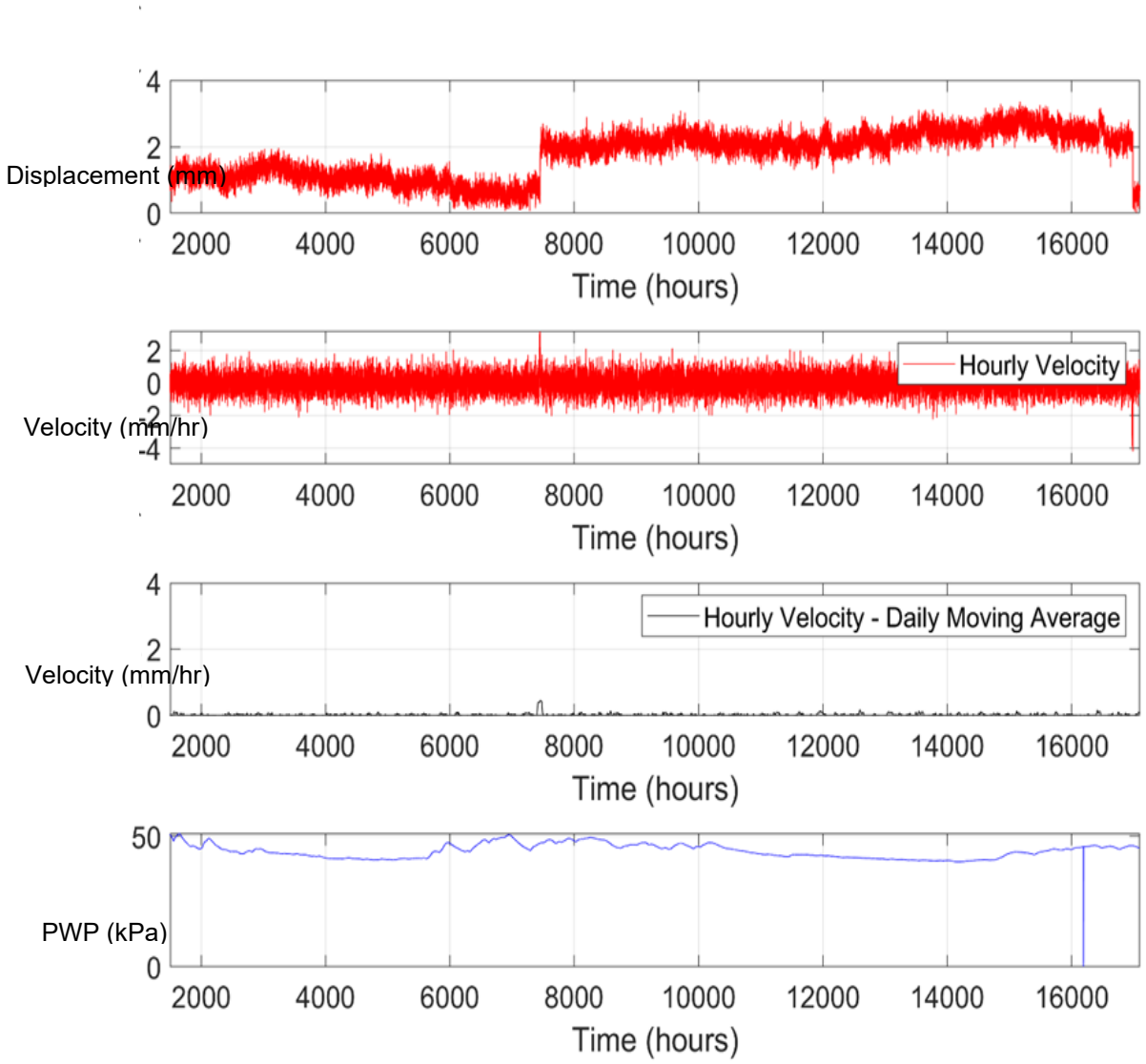

Figure 3.24: Monitored velocities and pore water pressures in the Spencer Creek South site. The discontinuity shown may reflect noise as no notable perturbation in groundwater was observed.

3.4.5 Spencer Creek North

Spencer Creek North has shown limited deformation since installation of borings in early 2017. It has, however, provided interesting insight into the rate of change in groundwater within the cemented seacliffs that comprise much of Oregon's Central Coast (Figure 3.25). Groundwater levels change rapidly after storm events, gradually dropping to steady state levels after period of modest rainfall. Throughout the wintertime, groundwater levels tend to stay elevated, eventually reaching steady state levels in the relatively dry summer and fall months. This data is directly useful for modeling the role of groundwater in cemented seacliffs along the Oregon Coast.

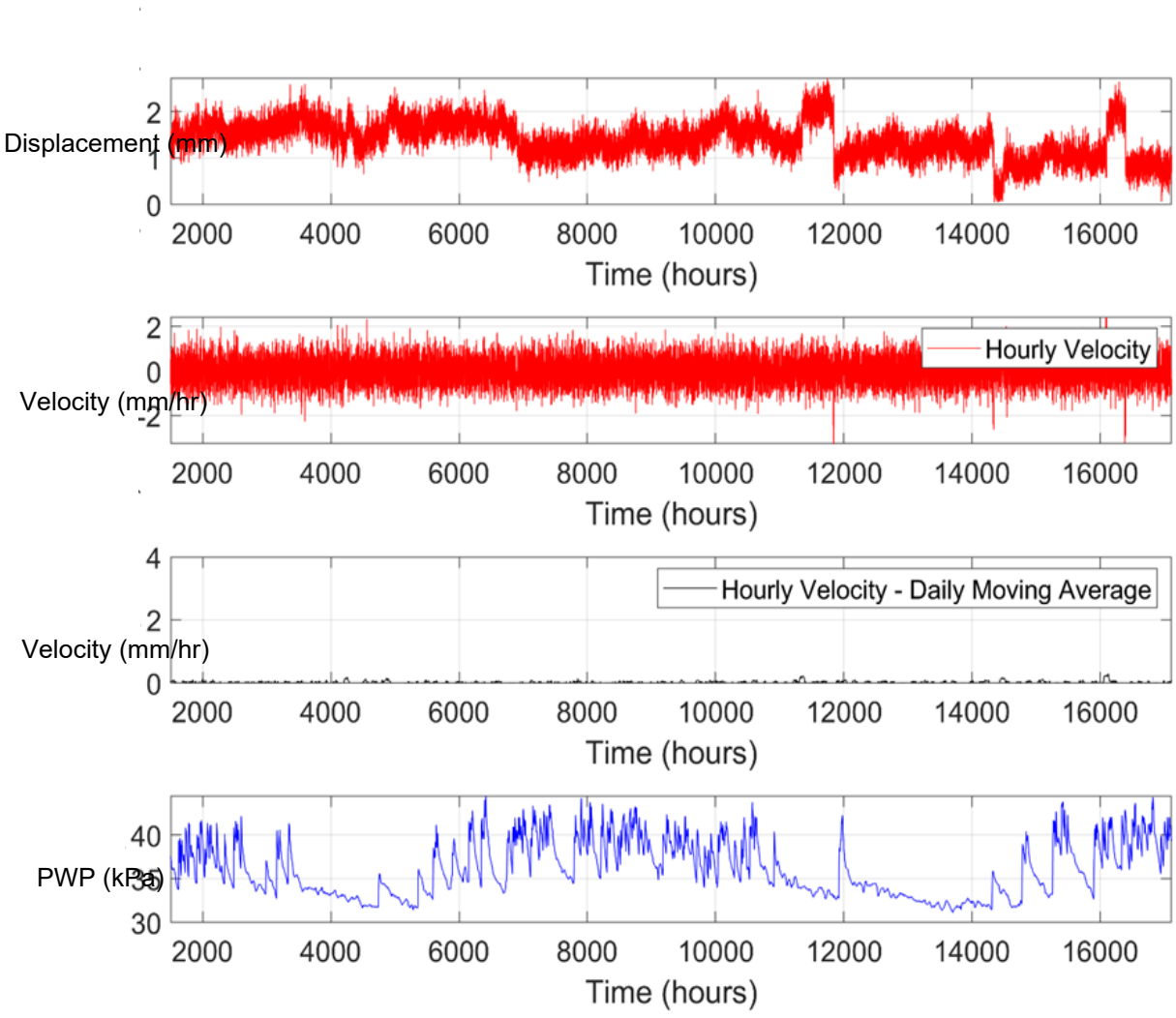

Figure 3.25: Monitored velocities and pore water pressures in the Spencer Creek North site.

3.4.6 Silver Point

Silver point has shown some activity in recent months (Figure 3.26), primarily as an expression of toppling (Figure 3.27) behind the major slump that daylights at the seacliff. This suggests recent, but intermittent activity of a seacliff failure at the site. Movement occurred during elevated levels of groundwater. However, groundwater levels have progressively increased at the site since monitoring without always being associated with ground movements. This likely suggests localized activity downslope of the boring may be driving the observed toppling response and extension upslope.

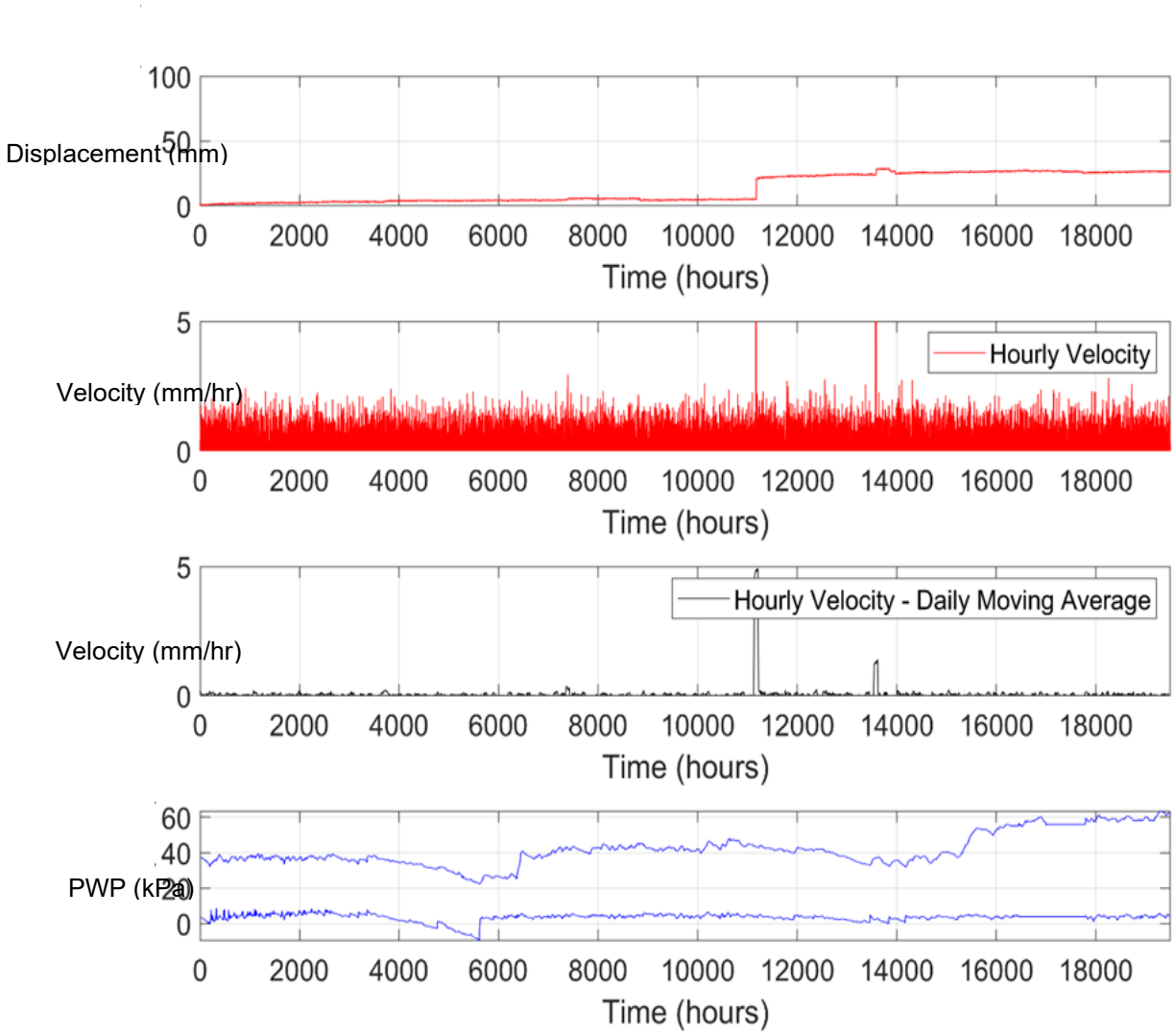

Figure 3.26: Monitoring data from Silver Point site.

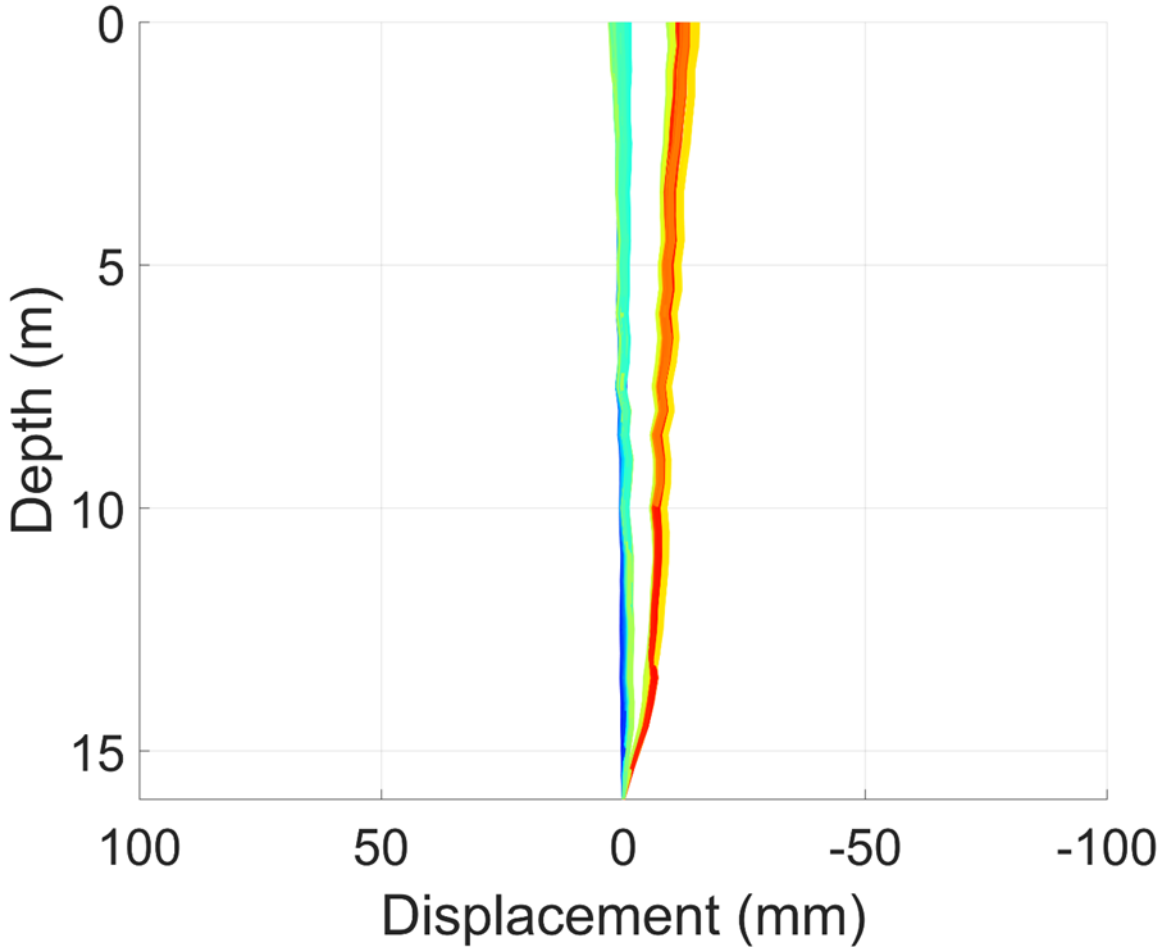

Figure 3.27: Measured shear profile at Silver Point site.

4.0 PROGRESSIVE FAILURE MODELING WITH CLIMATE VARIABLES

Thus far, we have developed two primary frameworks to assess the influence of coastal erosion impacts on (1) progressive landslide movements, and (2) seacliff retreat. Elements of the former work has been published in Leshchinsky et al. (2019), and some of its components and key findings described herein. The framework for seacliff retreat is still in development but has made major progress to date.

4.1 PROGRESSIVE LANDSLIDE MOVEMENTS

In the published study (Leshchinsky et al. 2019), a framework is presented that captures the coupled relationship between undercutting, pore pressure change, and progressive landslide movement. This model captures the evolution of landslide geometry (Figure 4.1) and undercutting rate and how these factors may influence observed landslide movements. Three of the test sites observed in this project were used as a basis for creating this model (Figure 4.2), including both Beverly Beach sites and the Arizona Inn landslide. Historical data regarding pore pressures and movements were used for geotechnical modeling (Figure 4.3), while reasonable rates of undercutting were estimated from repeat TLS capture at sites. Model outputs demonstrate that progressive landslides that have a smaller length to depth ratio are more sensitive to undercutting, particularly with increased erosion from wave attack (Figure 4.4). That is, with increased undercutting, landslides with small length to width ratios may realize a nonlinear increase in yearly movements with amplified erosion. Landslides with large length to width ratios demonstrate an increase in yearly movements with erosion but are much less sensitive. All landslides exhibited notable decreases with yearly movements if erosion was decreased or completely arrested. However, the primary driver of landslide movements, as expected, stemmed from increases in pore pressures associated with groundwater changes in wet months.

This study demonstrates that armoring or prevention of undercutting in progressive coastal landslides of modest size may significantly decrease yearly movements. Further, increased erosion may greatly exacerbate the activity of these landslides. Management of groundwater is critical for arresting all movements in these slope failures.

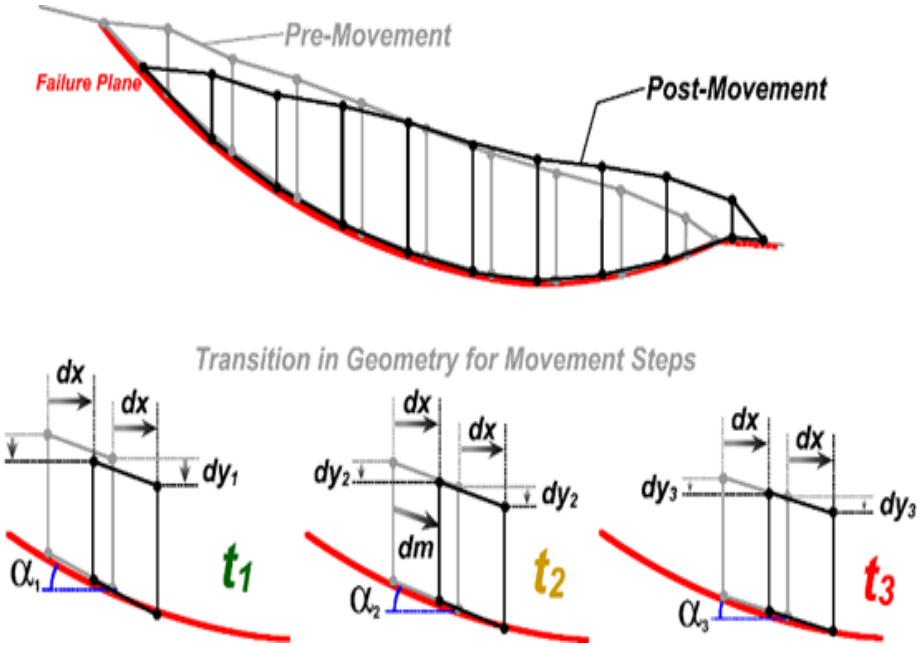

Figure 4.1: After Leshchinsky et al. (2019). Schematic of movement steps and notation.

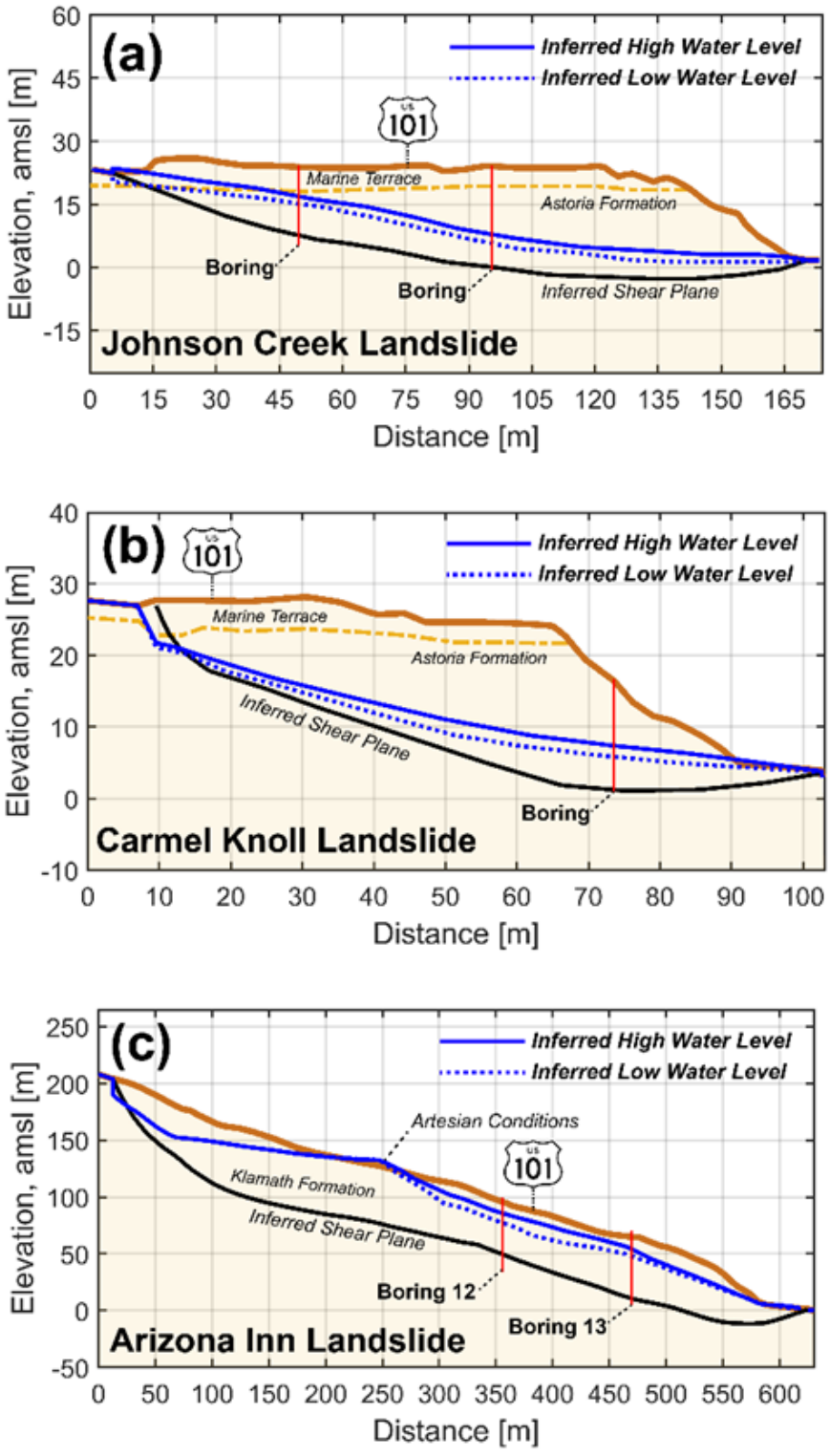

Figure 4.2: After Leshchinsky et al. (2019). Landslide and phreatic surface geometry for (a) Johnson Creek (after Schulz and Wang 2014); (b) Carmel Knoll (after Schulz and Wang 2014); and (c) Arizona Inn landslides (after ODOT, 1995).

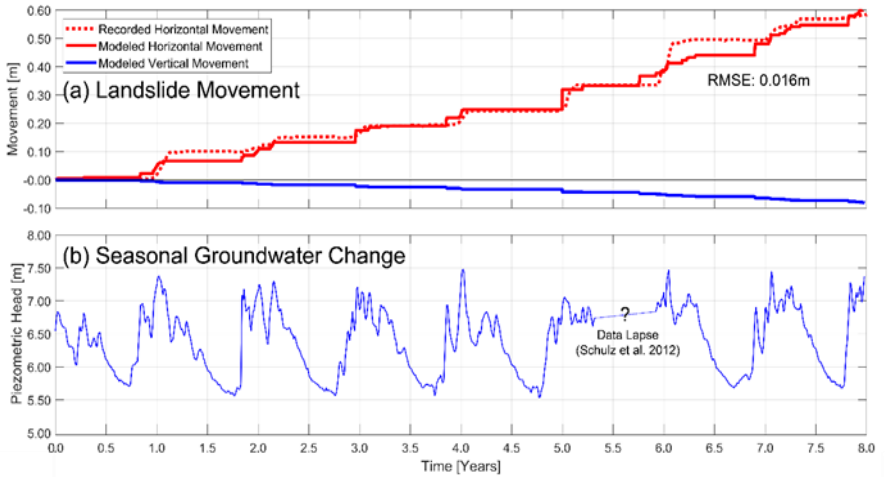

Figure 4.3: After Leshchinsky et al. (2019). (a) Modeled and measured landslide movement for the Johnson Creek Landslide and (b) measured piezometric head from January 2005 to January 2013 (after Schulz et al. 2014).

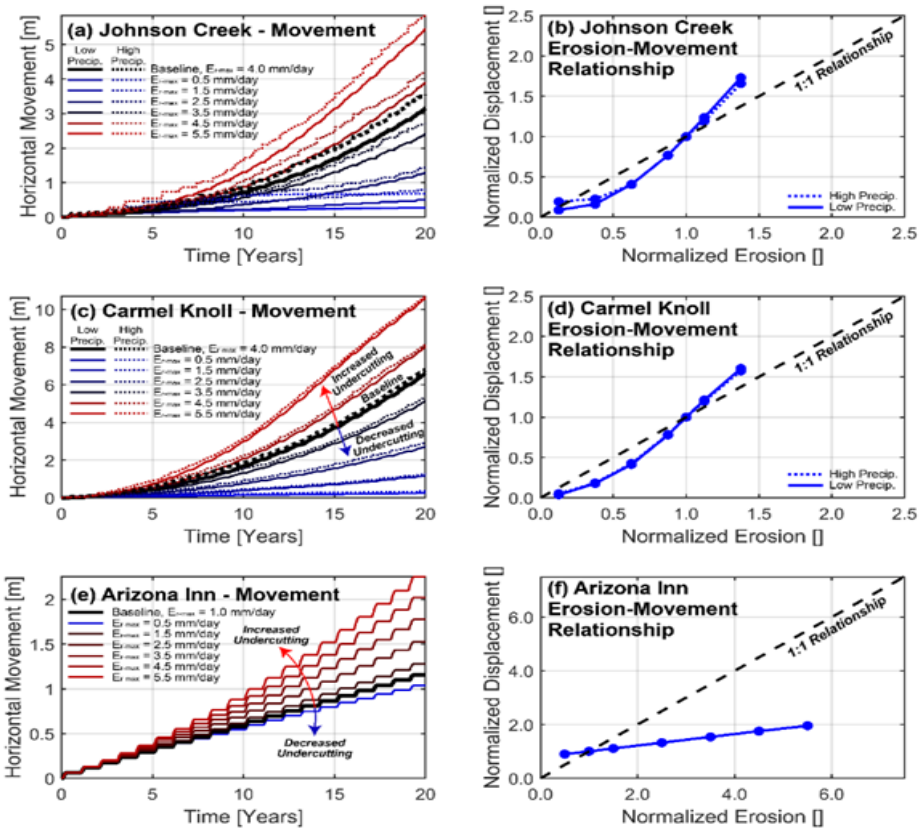

Figure 4.4: After Leshchinsky et al. (2019). Modelled landslide movements for select landslides over 20 years considering high and low precipitation conditions (dashed and solid lines, respectively) and various erosion rates (a) Johnson Creek; (c) Carmel Knoll; and (e) Arizona Inn. Inferred relationship between landslide movement and increased or decreased erosion after 20 years for select landslides (b) Johnson Creek; (d) Carmel Knoll; and (f) Arizona Inn.

4.2 SEA CLIFF RETREAT FROM COLLAPSE AND OVERHANG FAILURE

While wave undercutting amplifies the mass movements of large coastal landslides, it may significantly exacerbate the retreat of cemented coastal seacliffs, many of which have limited clearance from existing ODOT right-of-way. A framework has been created that imparts undercutting and assesses both (1) overhang failures, and (2) catastrophic slope failures (Figure 4.5). Each of these failures provides temporary self-armoring of a given sea cliff, which eventually erodes away. This feedback captures the general processes that dictate seacliff retreat and is easily generalizable to the sites monitored in this project. Inputs from repeat TLS collection (i.e. undercutting rates, erosion of failed material) may be directly used as inputs for this model. Undercutting rates and armor erosion rates may be amplified to appropriately capture potential effects of sea level rise and wave runup. Geotechnical parameters will be determined from forensic analysis of ongoing sea cliff failures.

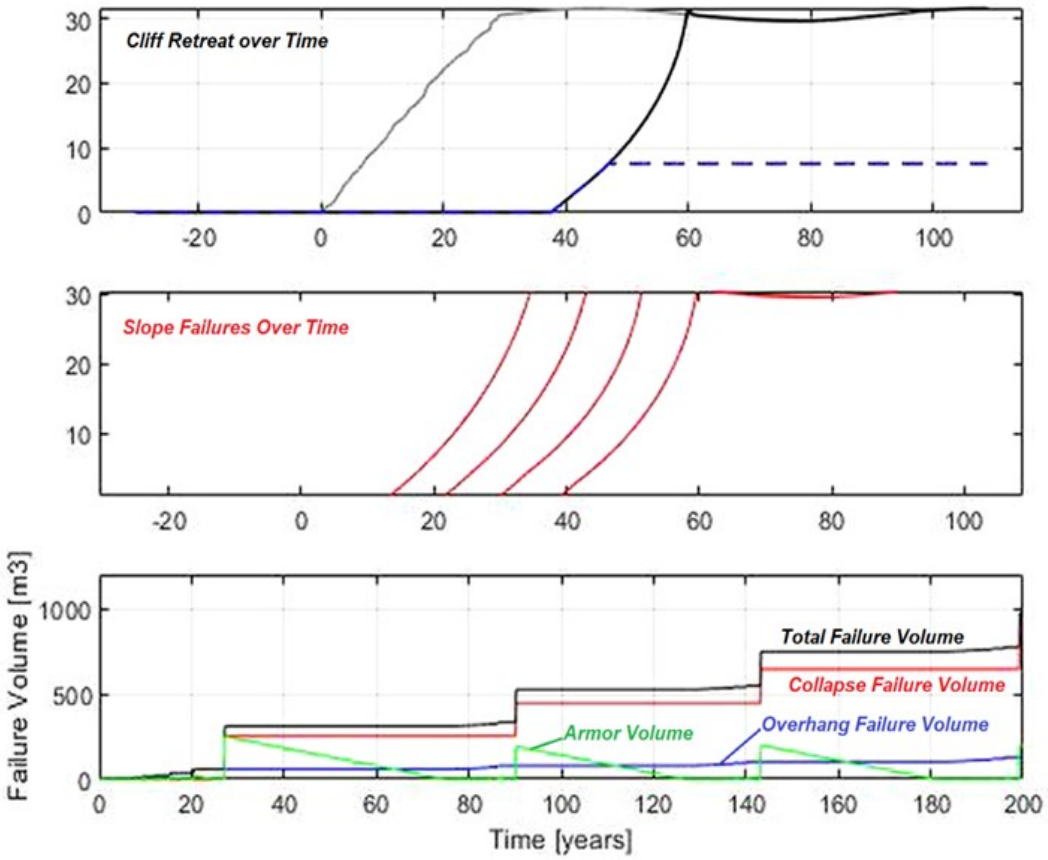

Figure 4.5: Model of sea cliff retreat considering overhang failures, collapse failures, and self-armouring. The retreat of the sea cliff over 200 years is shown in the top figure, with the grey line representing initial conditions and the black line representing final conditions. Retreat over this time period and soil conditions is approximately 35 meters.

4.3 EXAMPLE RESULTS/SCENARIOS

Both models can and will be primed to account for potential increases in erosion stemming from sea level rise and increased wave attack.

The normalized relationships proposed in Figure 4.4 are generalized so relative changes in erosion may be used to directly assess how changes in sea cliff erosion rates influence landslide movements. These results may be interpolated to assess relative changes in landslide movements for progressive failures along the Oregon Coast. Ongoing assessment of erosion behavior from repeat TLS collection can inform existing erosion rates in comparison to normalized relationships presented to infer sensitivity of landslide movements to sea cliff erosion. The normalized relationships between erosion and mass movement, along with a variety of length to depth ratios will provide simple, generalizable outputs to a variety of landslide conditions, just as shown in Figure 4.4. Ongoing monitoring will provide updated erosion rates over time, along with changes in potential movement.

Erosion rates from TLS will also be used to inform baseline dynamics governing seacliff retreat. As these input parameters may be directly assessed, baseline coastal retreat can be assessed and a retreat rate may be determined explicitly (for example, in Figure 4.5, the retreat rate is 0.18 m/year). Increases in undercutting and erosion may also be directly assessed, providing a range of potential retreat rates considering a variety of erosion scenarios. Armored conditions will also be assessed to highlight the potential influence of mitigation systems on coastal retreat. As this framework is sensitive to seacliff geometry, these conditions will be evaluated for multiple cross-sections of each site, as well as a variety of normalized geometric parameters (soil shear strength, cliff heights, and erosion rates) to allow simple generalization of outputs for planning. For the monitored sites, numerous cross-sections will be analyzed to establish cliff retreat based on site-specific monitored erosion rates. That is, for each cross-section, retreat may be assessed considering baseline, increased or decreased erosion rates. This will be done for each cross-section, enabling visualization of potential shoreline locations in coming decades. This will also provide spatial context to the threat of seacliff retreat with respect to ODOT right-of-way.

4.4 FUTURE DEVELOPMENTS TO THE MODEL

Both of the proposed scenario frameworks reflect the deleterious effects of coastal undercutting on slope instabilities. The progressive landslide work may be modified to reflect more conditions and a wider array of landslides as data becomes available. The work on coastal retreat will be bolstered by forensics of sea cliff failures and comparison of actual sea cliff geometry to modeled conditions. Once validation is achieved, coastal retreat considering temporal and spatial variations in mechanical properties and stability will be considered.

Advances to the hydrological aspects of the model will also be implemented. These could include inputs of precipitation from NOAA or PRISM, tidal data from NOAA, or wave activity from wave buoys to consider significant wave heights, wave direction, and wave period. This information can also be combined with the geometric data provided by lidar to compute wave contact hours and runup.

Currently the model code is written to analyze a single, representative cross section. However, we are developing code to extract cross sections and other important geometric properties from the lidar data in RAMBO as input into the model code so that a large section of coastline can be analyzed. Python scripts will then be developed to import these results into a geodatabase in ArcGIS software such that the data can be combined with asset data for targeted risk assessment and climate change adaptation planning.

5.0 BENFITS TO ODOT AND IMPLEMENTATION

This project has both short-term benefits already realized in the life span of the project as well as benefits that will continue beyond the life of the project.

5.1 SHORT TERM

Several short-term benefits have been identified since the start of the project, including:

- The data collected for Hooskanaden for this research project played an immediate role in ODOT's response to the large failure of Highway 101 at Hooskanaden. By having baseline data in place from this project, additional surveys could be rapidly conducted such that displacement vectors could be quickly obtained to show the magnitude and distribution of movement across the site. The UAS lidar data also was used by ODOT Geometronics to minimize the amount of field survey work needed in the difficult terrain, enabling designers to begin work on a new alignment much sooner after the event. The UAS orthophotos and UAS lidar data were also immediately used by region 3 Geologists.

- The research methodology document provides guidelines to help ODOT with establishing monitoring programs for other sites in the future. The guidance and demonstrated success of utilizing new technologies such as UAS lidar, RTK UAS SFM/MVS surveys, and MEMs sensors are applicable to a wide range of monitoring projects beyond coastal erosion and landslide studies. The project team has had numerous conversations with ODOT personnel regarding these technologies and lessons learned.

- Presentations have also been given at the Engineering ODOT Geotechnical and Geology Technology Transfer Meetings. In both 2017 and 2019, the research team has shared relevant research results with ODOT personnel at these technology transfer meetings.

- Developed analysis code including code and scripts to process and analyze terrestrial lidar data, code for logging and transmitting sensor data from the in-situ instrumentation, and code to analyze progressive failures.

5.2 LONGER TERM BENEFITS

ODOT needs a coordinated program to establish the system and tools needed to initiate, manage, and analyze data assessing coastal landslide and erosion risks. The findings from this project will enable ODOT to:

- Relate climate events to site conditions, changes, and risk levels. Results from this project will also inform climate impacts to groundwater changes, their effects on

landslide movement, and to differentiate these effects from those related to coastal erosion rates at the most vulnerable sites.

- Utilize advanced methods for geotechnical investigation and monitoring of landslides that can subsequently be adapted for common agency practice resulting in more accurate and efficient landslide monitoring and mitigation efforts, particularly from loss of sea cliff support due to erosion.

- Respond quicker (and possibly before) emergency events. Having a program in place with supporting long term baseline data at priority sites will also help ODOT predict and identify when specific sites will show/are showing heightened levels of distress and corrective action may be warranted before an impending failure occurs to minimize risk to the travelling public as well as ODOT personnel.

- Systematically analyze long sections of coastline adjacent to Highway 101 to identify priority sites and future trends. ODOT can also utilize this information in planning to evaluate the potential impacts of potential mitigation techniques and future scenario events. The analysis framework also allows ODOT to analyze other sections of highway facing similar hazards such as river or stream erosion, failure of cut slopes, etc.

- Evaluate the effectiveness of mitigation techniques. ODOT could use the tools developed in this research to monitor sites with mitigation and adjacent sections of coastline. A major challenge in seacliff erosion mitigation techniques is that they often result in accelerated erosion adjacent to the mitigated slope.

- Understand how coastal erosion affects retreat of bluffs in the mid- and long-term, particularly in context of the location of vulnerable ODOT right-of-way. By characterizing actual evolution of seacliff morphology with erosion with monitoring, we may project volumes of cliff collapse and retreat of bluffs with and without mitigation. This may guide strategic mitigation efforts.

5.3 IMPLEMENTATION

This research would be used by ODOT to inform project-level risk and decision making where coastal infrastructure is threatened by landslides and erosion. It will also inform planning and land-use at a policy-level regarding shoreline protection where infrastructure is threatened by future sea cliff retreat. Improved projections of timing for infrastructure damage or loss provides ODOT with information needed to make informed decisions regarding shoreline protection planning of public property or adaptation strategies at the policy-level. Further, this research could be used by the agency to justify exceptions to land use goals and other environmental restrictions when proposing construction projects to protect infrastructure. This includes exceptions to Statewide Goal 18 (Beaches and Dunes) regulated by the Department of Land Conservation and Development and coastal permits issued through the Oregon Parks and Recreation Department.

6.0 REFERENCES

Dunham, L., Wartman, J., Olsen, M. J., O'Banion, M., & Cunningham, K. (2017). Rockfall activity index (RAI): A lidar-derived, morphology-based method for hazard assessment. *Engineering Geology*, *221*, 184–192. https://doi.org/10.1016/j.enggeo.2017.03.009

Leshchinsky, B., Olsen, M. J., Mohney, C., Glover-Cutter, K., Crook, G., Allan, J., . . . Mathews, N. (2017). Mitigating coastal landslide damage. *Science*, *357*(6355), 981–982. https://doi.org/10.1126/science.aao1722

Leshchinsky, B., Olsen, M. J., Mohney, C., O'Banion, M., Bunn, M., Allan, J., & McClung, R. (2019). Quantifying the sensitivity of progressive landslide movements to failure geometry, undercutting processes and hydrological changes. *Journal of Geophysical Research: Earth Surface*, *124*(2), 616–638. https://doi.org/10.1029/2018jf004833

ODOT: Oregon Department of Transportation (1995). Phase II: Arizona Inn Landslide geotechnical investigation, Region 3 Office, Curry County, Oregon

Olsen, M.J., Allan, J.C., & Priest, G.R. (2012), *Movement and erosion quantification of the Johnson Creek, Oregon landslide through 3D laser scanning.* Oakland, CA: ASCE GeoCongress. Retrieved from https://ascelibrary.org/doi/pdf/10.1061/9780784412121.312

Schulz, W. H., & Wang, G. (2014). Residual shear strength variability as a primary control on movement of landslides reactivated by earthquake-induced ground motion: Implications for coastal Oregon, U.S. *Journal of Geophysical Research: Earth Surface*, *119*(7), 1617–1635. https://doi.org/10.1002/2014jf003088